의학박사 학위논문

Activation mechanisms of eNOS expressed in pulmonary artery smooth muscle cells

폐동맥 평활근세포에 발현된 내피세포형 산화질소 합성효소의 활성화 기전

2016 년 08 월

서울대학교 대학원

의과학과 의과학전공

김 혜 진

A thesis of the Degree of Doctor of Philosophy

폐동맥 평활근세포에 발현된 내피세포형 산화질소 합성효소의 활성화 기전

Activation mechanisms of eNOS expressed in pulmonary artery smooth muscle cells

August 2016

The Department of Biomedical Sciences,
Seoul National University
College of Medicine

Hae Jin Kim

폐동맥 평활근세포에 발현된 내피세포형 산화질소 합성효소의 활성화 기전

지도교수 김 성 준

이 논문을 의학박사 학위논문으로 제출함

2016 년 6 월

서울대학교 대학원
의과학과 의과학전공
김 혜 진

김혜진의 의학박사 학위논문을 인준함
2016 년 6 월

위 원 장 _____ (인)
부위원장 _____ (인)
위 원 _____ (인)
위 원 _____ (인)
위 원 _____ (인)

Activation mechanisms of eNOS expressed in pulmonary artery smooth muscle cells

by

Hae Jin Kim

A thesis submitted to the Department of Biomedical Sciences in partial fulfillment of the requirements for the Degree of Doctor of Philosophy in Medical Science at Seoul National University College of Medicine

June 2016

Approved by Thesis Committee:

Professor _____Chairman
Professor _____Vice chairman
Professor
Professor
Professor

ABSTRACT

Pulmonary arteries (PAs) have a high degree of compliance, which is critical for buffering the wide ranges of blood flow. Here, I aimed to address a hypothesis that PA smooth muscle cells (PASMCs) express endothelial nitric oxide synthases (eNOS) that might be activated by mechanical stress and vasoactive agonists. In the myograph study of endothelium-denuded rat PAs, NOS inhibition (L-NAME, 100 μM) induced strong contraction (96 % of 80 mM KCl-induced contraction (80K)) in the presence of 5 nM U46619 (thromboxane A_2 (TXA_2) analogue) with relatively high basal stretch (0.3 g, S(+)). With lower basal stretch (0.1 g, S(-)), however, L-NAME application following U46619 (TXA_2/L-NAME) induced weak contraction (27 % of 80K). Inhibitors of nNOS and iNOS had no such effect in S(+) PAs. In endothelium-denuded S(+) mesenteric and renal arteries, TXA_2/L-NAME-induced contraction was only 18 % and 21 % of 80K, respectively. Expression of endothelial-type NOS (eNOS) in rat PASMCs was confirmed by RT-PCR and immunohistochemistry. Even in S(-) PAs, pretreatment with H_2O_2 (0.1 - 10 μM) effectively increased the sensitivity to TXA_2/L-NAME (105 % of 80K). Patch clamp experiment

showed that H_2O_2 facilitated membrane stretch-activated cation channels (SACs) in rat PASMCs. Consistently, mechanosensitive cation channel inhibitors (GxMTx4 and DIDS) effectively eliminated SAC activity in PASMCs and also TXA_2/L-NAME contraction in S(+) PAs. *Vice versa*, NADPH oxidase inhibitors, reactive oxygen species scavengers (Tiron and PEG-catalase), or an Akt inhibitor (SC-66) suppressed TXA_2/L-NAME-induced contraction in S(+) PAs. In a human PASMC line (PCS-100-023, ATCC), immunoblot analysis showed the following: 1) eNOS expression, 2) Ser^{1177} phosphorylation by U46619 and H_2O_2, and 3) Akt activation (Ser^{473} phosphorylation) by U46619. Taken together, the muscular eNOS in PAs can be activated by TXA_2 and mechanical stress via H_2O_2 and Akt-mediated signaling, which may keep those balance to the contractile signals from TXA_2 and mechanical stimuli. Interestingly, both in monocrotaline (MCT)- and chronic hypoxia (CH) -induced pulmonary arterial hypertensive rats, TXA_2/L-NAME contraction of the S(+) PAs were largely decreased. The eNOS activated in PASMCs could counterbalance an excessive vasoconstriction, lowering the workload to the right heart.

Pflugers Arch (2016) 468(4):705-16. Published.

Keywords: pulmonary artery smooth muscle, eNOS, stretch, Thromboxane A_2, hydregen peroxide

Student number: 2011-21938

CONTENTS

LIST OF TABLES AND FIGURES

ABBREVIATIONS

PA: Pulmonary artery

PASMC: Pulmonary artery smooth muscle cells

NOS: Nitric oxide synthase

EDRF: Endothelium derived relaxing factor

EDR: Endothelium dependent relaxation

TXA_2: Thromboxane A_2

L−NAME: L−N^G−Nitroarginine methyl ester

$PGF_{2\alpha}$: Prostaglandin $F_{2\alpha}$

ACh: Acetylcholine

MA: Mesenteric artery

RA: Renal artery

ROS: Reactive oxygen species

SAC: Stretch activated cation channels

NOX: NADPH oxidase

PAH: Pulmonary arterial hypertension

MCT: Monocrotaline

CH: Chronic hypoxia

INTRODUCTION

Characteristics of pulmonary circulation

Pulmonary circulation is the movement of blood from heart to the lungs for oxygenation, then rotate back to the heart again. In general, the average stroke volume of humans in right ventricle is 5 liters per minute as blood flow of systemic circulation. However, pulmonary arterial pressure maintains about 12 mmHg lower than that of systemic arterial pressure (West, 2007). Furthermore, another feature in pulmonary vascular is lower resistance less than one-tenth of systemic vascular resistance. It means that pulmonary vascular resistance decreases dramatically, allowing pulmonary blood flow to increase. For example, even though cardiac output during exercise increases up to 300 % mean pulmonary arterial pressure increases 50 % only. It is achieved by recruiting non-perfused vessels and distending perfused vessels due to high compliance. Both responses are generally ascribed to passive changes in non-muscular capillaries (Lumb and Nunn, 2005). However, active regulation of the tone of pulmonary arteries (PAs) may also play a role in this low vascular resistance. For instance, nitric oxide (NO) from the endothelium could induce a state of active

vasodilation in the PA (Cooper et al., 1996). Several papers has been coming up for existence of NOS in smooth muscle (Buchwalow et al., 2002; Han et al., 2013). However, the possibility of eNOS expression in PASMCs and their potential roles have not been investigated yet.

Lack of myogenic response in PAs

Pulsatile blood flow generated dynamic mechanical forces and shear stress influences constantly to pulmonary wall, which is important to regulate of vascular structure, myogenic tone, and functional responses to vasoactive molecules (Birukov, 2009; Thacher et al., 2010). Vascular cells have the ability to discern changes by mechanical forces and act as mechanotransduction. One of the mechnosensors, stretch-activated cation channels (SACs) has been studied in rabbit and rat PASMCs (Ducret et al., 2010; Park et al., 2003; Park et al., 2006). The depolarizing influence of SACs and subsequent activation of L-type voltage-operated Ca^{2+} channels ($VOCC_L$) increase the cytosolic Ca^{2+} concentration ($[Ca^{2+}]_c$) in PASMCs (Bialecki et al., 1992). SACs in systemic arterial myocytes underlie the myogenic contractile response to increases in transluminal pressure, which in turn

influences total peripheral resistance (Baek and Kim, 2011; Hill et al., 2006). Despite the presence of SACs in PASMCs, the existence of a myogenic response in the normal PAs has been generally denied (Belik, 1994; Naik et al., 2005), which might imply the presence of myogenic relaxing signals counterbalancing the influence from SACs.

Essential roles of TXA_2 receptors in PA physiology

Intrinsic agonists such as TXA_2 activating TXA_2 receptors (TPs) induce potent constriction of the PAs (Huang et al., 2004). TP receptors are known to couple to G protein receptor to stimulate the DAG/IP_3 second messenger system (Breyer et al., 2001). Increases of $[Ca^{2+}]_i$ by TXA_2 in PASMCs are associated with a PKC-mediated inhibition of Kv channels (Cogolludo et al., 2003). Also, TP-mediated contraction of vascular smooth muscle partly depends on the influx of extracellular Ca^{2+} through both L-type Ca^{2+} channels at micromolar level of TXA_2 and non-selective cation channels at nanomolar level of TXA_2 (Tosun et al., 1998; Yoo et al., 2012).

Circumferential stretching of the PA is reported to induce thromboxane A_2 (TXA_2) release from the endothelium,

augmenting vessel tone (Nakayama et al., 1997). In the PAs, minimum levels of TXA_2 appears to be a physiological condition because the pretreatment with nanomolar TXA_2 was indispensable for the hypoxic pulmonary vasoconstriction (HPV) in the isolated PAs (Park et al., 2011; Yoo et al., 2012). However, without concomitant relaxing signals, the PAs with low perfusion pressure are prone to collapse only by moderate contractile responses and agonists *in vivo*.

Vasorelaxing roles of nitric oxide (NO)

NO formed from L-arginine by NOS is known as a potent vasodilator in various type of cells. The endothelium is generally believed to be the site of endothelial-type NOS (eNOS or NOS3) expression, and responsible for NO-cGMP-PKG pathway as an endothelium-derived relaxing factor (EDRF) (Michel and Vanhoutte, 2010). The activity of eNOS is mainly regulated by increased $[Ca^{2+}]_c$ in the calmodulin (CaM)-dependent manner. In addition to the conventional Ca^{2+}/CaM-dependent pathway, various signaling mechanisms such as phosphorylation (e.g. Ser^{1177}) participate in the fine modulation of eNOS activity (Fleming, 2010). Alterations of eNOS activity affect vascular

tone (Dikalova et al., 2010; Earley and Walker, 2003) and induce pathological responses such as hypertension (Evora et al., 2012; Kietadisorn et al., 2012), which is also true in the PA (Barbera et al., 2001; Mathew et al., 2007; Sedoris et al., 2009).

Regarding the lack of myogenic responses and the necessity of intrinsic express nitric oxide synthase (NOS) that is widely responsible for the vasorelaxing signals. Shear stress in the endothelium is known to stimulate NO signaling (Fleming, 2010; Kumar et al., 2010; Michel and Vanhoutte, 2010). However, to maintain the low resistance and high compliance of the inter- and intra-lobar PA with multiple layers of myocytes in the media, relaxing mechanisms intrinsic to the smooth muscle would also be necessary.

Previous studied of NOS in vascular smooth muscle

Although the expression of NOS, especially the eNOS, is generally localized to the endothelial cells in the vascular system, there are also reports suggesting the expression of NOS in the medial layer of arteries (Buchwalow et al., 2002) Subsequent studies suggested that NO from myogenic NOS may induce vasorelaxation in endothelium-deprived arteries when

stimulated with a pharmacological cocktail of acetylcholine (ACh) and superoxide scavenger, Tempol (Buchwalow et al., 2008; Cacanyiova et al., 2013). In addition, it has been recently found that skeletal arterial smooth muscles also express eNOS that appears to be stimulated by alpha-adrenergic stimulation of myocytes. Severe hypoxia inhibited the muscular eNOS to induce a potent augmentation of the alpha adrenergic contraction (Han et al., 2013). However, the physiological roles of muscular and regulatory signals of NOSs are not understood in PAs.

Goals of the study

The low resistance of pulmonary circulation under the large fluctuation of circulating blood volume is generally known to be due to the recruitment of previously collapsed branches of PAs (Fig. 1, upper models). In addition, further increase of PA diameters would occur (Fig. 1, lower models). In the process of distension, an active relaxation mechanisms such as eNOS might be activated. Here I hypothesize that PASMCs may express NOS that can be activated in response to mechanical stretching and physiological agonists such as TXA_2. To investigate this hypothesis, endothelium-denuded PA rings were prepared for

myograph and molecular biological assay.

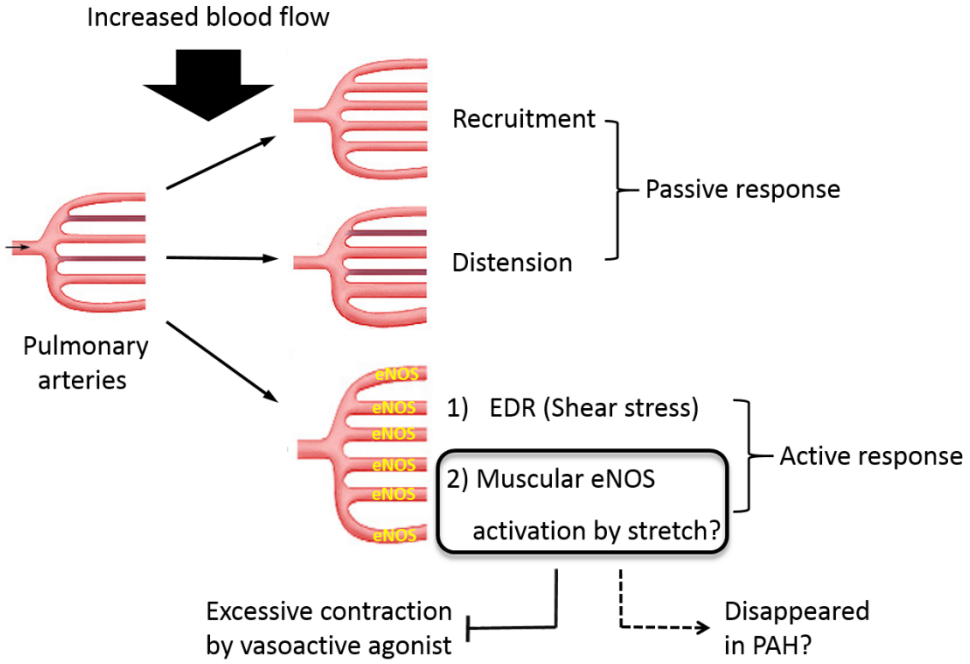

Figure 1. A hypothetical model of pulmonary arteries response to high blood flow.

MATERIALS AND METHODS

1. Animals and PAH models

8 week-old Sprague-Dawley (SD) male rats were used in this study (230-260 g). All procedures of animal experiments were conducted in accordance with the Guide for the Care and Use of Laboratory Animals published by the US National Institutes of Health (8^{th} Edition, revised 2011), and also conformed to the Institutional Animal Care and Use Committee (IACUC) of Seoul National University (IACUC approval No.: SNU-111129-1-1).

8 week-old male SD rats received a single subcutaneous injection of saline (60 mg/kg) or MCT (60 mg/kg) and were allowed 21 days to develop pulmonary hypertension.

The hypoxic chamber with an oxygen gas controller (Proox Model 110, Bioshperix., USA) was used to control oxygen levels. The oxygen level was adjusted using 100 % N_2 gas injection. In the chamber, a circulating fan was operated and carbon dioxide absorbent was added to protect from hypercapnia. To maintain humidity, silica gels were placed in bottom of chamber. 8 week-old SD male rats were initially exposed to an oxygen level (PO_2) of 10 - 12 % during the first week for adaptation. Then PO_2 was further lowered to 8 % during next 2 weeks.

2. Preparation of rat artery rings

Rats were fully anesthetized by intraperitoneal injection of pentobarbital sodium (60−100 mg/kg) and euthanized by cervical dislocation. Their lungs were then quickly placed Normal Tyrode (NT) solution. The NT solution was contained (in mmol/l): 140 NaCl, 5.4 KCl, 0.33 NaH2PO4, 10 HEPES, 10 glucose, 1 CaCl2 and 1 MgCl2, pH 7.4 titrated with NaOH. The second and third PA branches from left upper lobe were dissected (inner diameter 150~250 ㎛) and cut into segments (3 mm long). Mesenteric arteries and renal arteries were prepared in the same way. The endothelium was denuded by gently rubbing the lumen with tungsten wire.


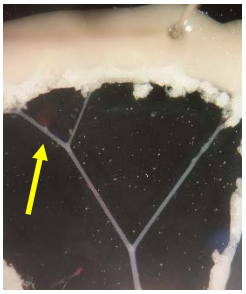


3. Isometric tension measurement

The segment arteries were mounted on 25 ㎛ wires in a dual−wire myograph system (620M; DMT, Aarhus, Denmark). The chambers of the myograph were filled with physiological salt

solution (PSS) contained (in mmol/l): 118 NaCl, 4 KCl, 24 $NaHCO_3$, 1 $MgSO_4$, 0.44 NaH_2PO_4, 5.6 glucose, and 1.8 $CaCl_2$. and equilibrated with a normoxic gas mixture (21 % O_2, 5 % CO_2, N_2 balanced) at 37 ℃. The relationship between transluminal pressure and stretching determined using the DMT myograph was calculated using the modified Laplace equation.

$$P = {2\pi T}/{i.c.}$$

The internal circumference (*i.c.*) of vessels can be increased during myograph by increasing the wall tension (*T*). The *i.c.* of vessels was set as 150 and 200 ㎛ for the applied *T* of 0.1 g (S(−) PA) and 0.3 g (S(+) PA), respectively. The expected equivalent transluminal pressure (*P*) was calculated as 10 and 30 mmHg for S(−) and S(+) PAs with a length of 3.5 mm, respectively. For mesenteric and renal arteries, higher *T* (0.5 and 1 g) was applied to mimic the expected systemic *P* of 70 and 140 mmHg, respectively. To confirm the viability of arteries as well as to obtain a standard contraction, the response to 80 mM potassium solution (80K) was measured initially. In each vessel, endothelium−dependent relaxation (EDR) was evaluated by applying 10 μM acetylcholine (ACh) in the presence of vasoconstrictors (ex. $PGF_{2\alpha}$ and Phenylephrine; PhE)

4. Isolation of PASMCs

Dissected PAs were incubated in an initial digestion medium (1 mg/mL papain, 5 mg/mL bovine serum albumin (BSA), and 1.5 mg/mL dithiothreitol (DTT) in Ca^{2+} free-NT solution) for 10-15 min, then moved to a second digestion medium (3 mg/mL collagenase, 1.5 mg/mL BSA, and1.5 mg/mL DTT in Ca^{2+} free-NT solution) for 10 - 15 min. The isolated PASMCs were gently agitated by using a Pasteur pipette and stored in Karft-Brühe storage solution that contained (in mmol/l): 70 KOH, 50 L-glutamate, 55 KCl, 20 taurine, 20 KH_2PO_4, 3 $MgCl_2$, 20 glucose, 10 HEPES, and 0.5 ethylene glycol tetra-acetic acid (EGTA) adjusted to pH 7.3 with KOH.

5. Reverse transcriptase polymerase chain reaction (RT-PCR)

Total RNA was prepared from isolated rat PASMCs and total PAs using TRIzol extraction (Invitrogen, Carlsbad, CA). Specific primers for nNOS, iNOS, eNOS, PECAM-1, and GAPDH were summarized in Table 1. cDNA was amplified with 2X Taq premix (SolGent, Deagon, Korea) using a DNA thermal cycler (Bio-Rad Laboratories, Hercules, CA). The amplification conditions were:

95 ℃ for 10 min, followed by 35 cycles of 95 ℃ for 30 s, 68 ℃ for 30 s, and 72 ℃ for 1 min. The PCR products were electrophoresed on a 2 % agarose gel at 120 V in Tris-acetate-EDTA buffer and confirmed using EtBr.

6. Immunohistochemistry

PAs were fixed in 4 % paraformaldehyde, paraffin-embedded, and cut into sections. Endogenous peroxidase was quenched with 3 % H_2O_2 for 5 min at room temperature. The following primary antibodies were diluted in antibody diluents (Invitrogen, Grand Island, NY): monoclonal mouse anti-eNOS (BD Bioscience, CA, USA, 1:300 dilution used), polyclonal rabbit anti-iNOS (NOVUS Biologicals, CO, U.S.A, 1:300 dilution used), and monoclonal mouse anti-nNOS (Santa Cruz Biotechnology, TX, USA, 1:300 dilution used). Secondary antibodies (anti-mouse and anti-rabbit) were used with Dako Envision+ System-HRP (Dako, Glostrup, Denmark). For chromogenic reactions, I used 3,3'-diaminobenzidine chromogen and substrate buffer for 10 min at room temperature. Finally, the sections were washed in distilled water for 5 min, counterstained with Mayer hematoxylin for 15 s, washed again in distilled water, dehydrated with ethanol,

cleaned with xylene, and mounted.

7. Cell culture

A human pulmonary arterial smooth muscle cell line (PCS-100-023, American Type Culture Collection, Manassas, VA) cells were grown in Vascular Cell Basal Medium (American Type Culture Collection, Manassas, VA), supplemented with growth kit (5 % fetal bovine serum (FBS), 5 ng/ml rh FGF, 5 μg/ml Insulin, 50 μg/ml Ascorbic acid, 10 mM L-glutamine and 5 ng/ml rh EGF). Cells were maintained in a humidified incubator at 37 ℃ with 5 % CO_2.

8. Immunoblot analysis

To obtain total protein, the cultured human PASMCs (PCS-100-023) were harvested and suspended in homogenization buffer containing 50 mM Tris-HCl (pH 7.4), 100 mM NaCl, 5 mM EDTA, 1 % Triton X-100, and a protease/phosphatase inhibitor cocktail (Roche Diagnostics) for 1 h at 4 ℃. The samples were centrifuged at 13,000 $\times g$ for 15 min at 4 ℃. Protein concentration was determined by the Bradford assay. The protein samples were mixed with Laemmli sample buffer,

resolved by 8 % SDS-PAGE, and transferred to polyvinylidene difluoride membranes in 25 mM Tris, 192 mM glycine, 0.01 % SDS, and 20 % methanol. Membranes were blocked in 1×TBS containing 1 % Tween-20 and 5 % bovine serum albumin (blocking solution) for 1 h at room temperature with gentle rocking, and incubated overnight at 4 ℃ with anti-eNOS (BD Bioscience, CA, USA, 1:1000 dilution used), anti-eNOS Ser^{1177}, anti-Akt, anti-Akt Ser^{473}, (Cell signaling Technology, MA, USA, 1:1000 dilution used all) and β-tubulin (Cell signaling Technology, MA, USA, 1:1000 dilution used) primary antibodies followed by relevant secondary antibodies after washing. The signals were determined using ECL Plus Western blotting detection reagents (Amersham Biosciences) and detected by film exposure. The intensity of each band was measured using with ImageJ analysis software program.

9. Electrophysiology

Whole cell and cell-attached patch clamp experiments were performed with a patch-clamp amplifier (Axon Instruments, Foster City, CA). pCLAMP software v.10.2 and Digidata-1332A (Axon Instruments) were used to acquire data and apply

command pulses, respectively. Recordings were performed at room temperature (23−25 ° C). Patch pipettes with free−tip resistance of about 3.0−4.0 MΩ were used. The bath solution contained: 125 mM CsCl, 10 mM HEPES, 10 mM Glucose, 1.8 mM $CaCl_2$, and 0.5 mM $MgCl_2$ adjusted to pH 7.4 titrated by CsOH. The pipette solution for whole−cell recording contained: 145 mM CsCl, 10 mM HEPES, 1 mM $MgCl_2$, 3 mM MgATP, and 0.5 mM EGTA adjusted to pH7.25 titrated by CsOH. The pipette solution for cell−attached single channel recording contained: 140 mM CsCl, 10 mM HEPES, 2 mM EGTA, and 1 mM $MgCl_2$ adjusted to pH 7.4 with CsOH. The signals were filtered at 1 kHz and sampled at a rate of 5 kHz.

10. Histology

Heart were perfused with phosphate salt solution (PBS) and fixed by 4 % paraformaldehyde for 2 days at room temperature. Fixed heart tissues were embedded in paraffin and cut into sections and then stained with hematoxylin and eosin (H&E). Stained heart tissues were analyzed by computerized image analysis system (TissueFAXS 3.5−Slides program, TissueGnostics GmbH, Vienna, Austria).

11. Statistical analysis

Data were managed and analyzed using OriginPro 8 software (OriginLab Corporation Northampton, MA 0106, USA). Statistical results were expressed as the mean ± standard error of mean. A paired or unpaired Student *t*-test were used as appropriate to evaluate for significance, indicated with *P*-value of $*P < 0.05$, $**P < 0.01$, and $***P < 0.001$.

RESULTS

1. Expression of eNOS in pulmonary artery smooth muscle cells.

1-1. NOS inhibition augments TXA_2-induced PA contraction with basal stretch

At first, I tested whether different levels of pretone stretch affects the response to a general NOS inhibitior, L-NAME (L-N^G-Nitroarginine methyl ester) alone. PA rings were initially kept in a relaxed state for 5 min before applying different levels of basal stretch force, namely, 0.1 g (6.4 mmHg; S(-)) or 0.3 g (19.3 mmHg; S(+)), and then further incubated for 30 min. Application of 100 μM L-NAME alone had no effect on the basal tone of S(-) and S(+) PAs (Fig. 2A, n=5). In each vessel, 80 mM KCl was applied to confirm the standard contraction level by membrane depolarization (80K contraction), the amplitudes of which were not different between S(-) and S(+) PAs (Fig. 2B, 1.54 ± 0.16 g and 1.71 ± 0.15 g in 0.1 and 0.3 g pretone, respectively n=25). Also, I found that the contractile sensitivities to various levels of extracellular $[K^+]$ (20, 40, 60, and 120 mM of $[K^+]_e$) were similar between S(-) and S(+) PAs

when normalized to the 80K contraction in each vessel (Fig. 2C, n=8 respectively).

Pretreatment with a relatively low level of TXA_2 analogue (5 nM U46619) alone induced only a small increase of the basal tone of S(−) and S(+) PAs. Interestingly, addition of L−NAME to U46619−pretreated PAs induced tonic contraction equivalent to 27 % and 96 % of 80K contraction in S(−) (n=15) and S(+) (n=13) PAs, respectively (Fig. 3A, B, E, *** $P < 0.001$). I also tested the effects of another NOS inhibitor, L−N^G−monomethyl arginine citrate (L−NMMA, 100 μM), which showed the same results; higher contraction in S(+) than S(−) PAs (20 % (n=8) and 85 % (n=5) of 80K contraction in S(−) and S(+) PAs, respectively, *** $P < 0.001$) (Fig. 3C, D, E). In each PA tested, the deprivation of functional endothelium was confirmed by the absence of acetylcholine (ACh)−induced relaxation in the prostaglandin $F_{2\alpha}$ ($PGF_{2\alpha}$−induced maximum contraction state (Fig. 2A and 3A−D). Hereafter, the contraction induced by L−NAME application in the presence of 5 nM U46619 is abbreviated as TXA_2/L−NAME contraction.

Next, I examined TXA_2/L−NAME contraction in mesenteric arteries (MAs) and renal arteries (RAs). To mimic the wall

tension induced by the ranges of systemic blood pressure, basal stretch force of 0.5 g (S(−)) or 1.0 g (S(+)) was applied to the MAs and RAs. The functional absence of endothelium (i.e., no ACh−induced relaxation) was also confirmed in each MA and RA (Fig. 4A−D). In both MAs and RAs, 5 nM U46619 induced feeble contraction that were slightly augmented by 100 μM L−NAME (Fig. 4). The normalized TXA_2/L−NAME contractions in S(+) MAs (n=12) and S(+) RAs (n=10) were only about 20 % of 80K contraction (Fig. 4E). The TXA_2/L−NAME contractions of MAs and RAs appeared slightly higher in S(+), but this was statistically insignificant.

Since L−NAME is not selective to the three isotype of NOS, I tested the effects of nNOS− and iNOS−specific inhibitors to reveal pharmacological clues for the isotype of NOS associated with TXA_2/L−NAME in S(+) PAs. When PAs were treated with 500 nM S−methyl−L−thiocitrullin (SMTC; nNOS specific inhibitor) after U46619 pretone application, neither S(−) nor S(+) PAs showed significant contractile responses. (Fig. 5A, B; n=6 and n=4 for S(−) and S(+), respectively)(Furfine et al., 1994). Similarly, 5 μM N−(3−(aminomethyl) benzyl) acetamidine (1400W; iNOS inhibitor) did not induce any

contractile response in S(+) PAs (Fig. 5C, D; n=6 and n=7 for S(−) and S(+), respectively)(Garvey et al., 1997). By contrast, the final application of L−NAME to S(+) PAs induced robust contraction (*** $P < 0.001$)(Fig. 5).

The above results suggest that the expression of eNOS functionally activated by TXA_2 and PA wall stretch in endothelium denuded rat PAs. The inhibition of eNOS by L−NAME might have unveiled the strong contractile response of PAs to the combined stimuli of TXA_2 and mechanical stretch (Fig. 5E).

1−2. Verification of eNOS expression in PASMCs

In enzymatically isolated PASMCs, RT−PCR analysis showed the mRNA expression of eNOS and iNOS (Fig. 6A). In the same preparation, the mRNA of platelet endothelial cell adhesion molecule (PECAM−1, an endothelial cell marker) was absent, excluding a contamination of endothelial cells. Vice versa, a positive signal for PECAM−1 was confirmed in endothelium−intact total PA samples (Fig. 6B). The paucity of pure PASMCs available from rat PA segments did not allow Western blot analysis. Instead, immunohistochemistry showed a discernable eNOS−positive signal in the muscular layers of PAs, but not in

the corresponding layers of MAs and RAs (Fig. 6C, I, J). The endothelial layers of the tested arteries commonly showed a strong signal for eNOS. However, denuded PA was detected eNOS signal not in endothelial layers but in smooth muscle layers (Fig. 6F). The positive signals for nNOS and iNOS were not significant in PAs (Fig. 6G, H). Similar results were observed in a total of six rats. Thus, these results are reasonable to infer that eNOS exists in rat PASMCs and is activated by nanomolar TXA_2 combined with PA wall stretch.

2. Mechanisms of muscular eNOS activation in rat PASMCs.

2-1. Requirements of TXA_2/L-NAME contraction in S(+) PAs: ROS and stimulated TP receptor

Exposure to stretching in arterial smooth muscle generates ROS that play roles in a variety of signals and responses (Dick et al., 2013; Mata-Greenwood et al., 2005; Paravicini et al., 2012). ROS such as superoxide anions are immediately transformed into relatively stable H_2O_2, which is an important physiological signaling molecule in the cardiovascular system.

To elucidate the putative role of ROS in TXA_2/L-NAME contractions, I tested whether exogenously added H_2O_2 mimics the S(+) effect. In S(-) PAs, the application of micromolar ranges of H_2O_2 (0.1 - 10 μM) to a U46619-pretreated vessel did not induce significant contraction. However, the addition of L-NAME induced potent contraction equivalent to TXA_2/L-NAME contraction in S(+) PAs (Fig. 7A, B). Inversely, TXA_2/L-NAME contraction in S(+) PAs was significantly diminished by a membrane-permeable catalase (PEG-catalase; 352 U/ml, n=20) or by the ROS scavenger, Tiron (1 mM, n=11) (Fig. 7C-E). To sum up above results, increase of ROS by stretch and

U46619 stimulation were necessary in order to activate muscular eNOS in PAs.

However, under the treatment of 10 μM H_2O_2, an application of L-NAME only did not induce any contraction in S(+) PA (Fig. 8A). Then I tested whether a partial depolarization-induced Ca^{2+} influx might replace the requirement of U46619 for the TXA_2/L-NAME contraction in S(+) PAs. However, the partial contraction of S(+) PAs induced by 30 mM KCl (30K) was only weakly augmented by L-NAME (Fig. 8B). Next, I tested whether a partial depolarization could replace the higher pretone condition. To address this question, 20 mM KCl (20K) was applied to S(-) PAs. The 20K condition alone had no significant effect on S(-) PA tone, and the addition of U46619 caused only a small contraction (10 % of 80K contraction). Interestingly, final addition of L-NAME induced robust contraction similar to that of S(+) PAs (Fig. 8C, D).

2-2. Role of mechanosensitive cation channels in the ROS-dependent contraction of PAs

The above results imply that TXA_2 receptor (TP) stimulation and stretch-induced H_2O_2 effectively facilitate muscular eNOS activation. On the other hand, the absence of TXA_2/L-NAME

contraction in PEG-catalase- or Tiron-treated S(+) PAs suggested that not only eNOS activation but also the contractile signals are also stimulated by H_2O_2-dependent mechanisms. Also, the partial depolarization could substitute the S(+) condition for TXA_2/L-NAME contraction. Taken together, it was proposed that the S(+) and/or H_2O_2 might have activated cationic channels such as SACs.

To investigate whether the activity of SACs is affected by H_2O_2, a cell-attached (c-a) patch clamp study was carried out in enzymatically dispersed rat PASMCs. A negative pressure of 10-30 cmH_2O applied to the patch membrane rarely induced SACs (Fig. 9A, 2/25 c-a recordings). By contrast, inclusion of 10 μM H_2O_2 in the pipette solution markedly enhanced SAC activity (Fig. 9B, n=22 from 35 cells tested for c-a recordings). The slope conductance of SACs facilitated by H_2O_2 was 33 ± 3.9 pS (Fig. 9C, n=14). Such channel activity was not observed when monovalent cations in the pipette solution were replaced by N-methyl-D-glucamin ($NMDG^+$), a large organic cation (Fig 9D, top trace, n=15). GsMTx4 3 μM, a spider venom peptide that inhibits mechanosensitive cation channels (Bowman et al., 2007), inhibited SACs in PASMCs (Fig. 9D, left trace, n=13). 4,4'-

diisothiocyanatostilbene-2,2'-sulfonic acid (DIDS) is another SAC inhibitor in vascular smooth muscle (Lee et al., 2007; Park et al., 2006), and no SAC was observed with 30 μM DIDS in the pipette solution containing 10 μM H_2O_2 (Fig. 9D, right trace, n=12). Then, the physiological role of SACs was tested in a myograph experiment. In S(+) PAs, pretreatment with GsMTx4 (*** $P < 0.001$, n=5) or DIDS (*** $P < 0.001$, n=6) effectively suppressed TXA_2/L-NAME contraction (Fig. 10).

2-3. Signaling mechanism of the muscular eNOS phosphorylation in S(+) PAs

Application of NOX inhibitors (10 μM VAS2870 or 100 μM Apocynin; n=9 and n=12, respectively) also suppressed TXA_2/L-NAME contraction in S(+) PAs (Fig. 11A, B). As for a downstream signal of the increase in H_2O_2, Akt-dependent phosphorylation of eNOS has been reported (Thomas et al., 2002). Pretreatment with 10 μM SC-66, an Akt inhibitor, effectively suppressed TXA_2/L-NAME contraction in S(+) PAs (Fig. 11C, D).

Ser^{1177} is a representative residue of Akt-dependent phosphorylation to activate eNOS (Fleming, 2010). I examined the phosphorylation of muscular eNOS by treatment with 5 nM

U46619 and 10 μM H_2O_2. Because the amount of purely isolated smooth muscle cells available from rat PAs was not sufficient for the immunoblot assay, a cultured human PASMC line (PCS-100-023, ATCC) was used. Both eNOS and Akt proteins were detected in human PASMCs under basal conditions, while little phosphorylation of eNOS Ser^{1177} was detectable in control cells. After treatment with 5 nM U46619 for 15 min, phosphorylation of Ser^{1177} was observed, which was significantly augmented by addition of 10 μM H_2O_2 during the final 10 min of U46619 treatment (Fig. 12A, B; $* P < 0.05$). Akt requires phosphorylation of Ser^{473} residue to become activated (Chen et al., 2001). Interestingly, 5 nM U46619 alone induced significant phosphorylation of Akt Ser^{473} (Fig. 12A, C, *** $P < 0.001$) However, it was not augmented by the additional application of 10 μM H_2O_2 (Fig. 12A, C; $P > 0.05$, n=4).

3. Disappearance of muscular eNOS function in pulmonary hypertension model rats

Monocrotaline (MCT), a pyrrolizidine alkaloid, is widely used to induce pulmonary arterial hypertension (PAH) in rats. It is known that an intraperitoneal (i.p.) injection of MCT causes toxicity in pulmonary endothelial cells, and subsequent inflammatory response induce PAH in three weeks (Dumitrascu et al., 2008; Pak et al., 2010). Another widely used PAH rodent model is made by incubation under chronic hypoxia (CH) conditions. The CH-PAH rat models mimic pulmonary hypertension associated with lung disease (Pak et al., 2010) and are characterized by a sustained increase in pulmonary arterial pressure (Cahill et al., 2012).

Both MCT- and CH-PAH models were made to investigate whether the TXA_2/L-NAME contraction is affected in the PAs (Fig. 1). To validate whether PAH was actually generated, the right ventricle wall thickness was compared between control and the PAH rats. A representative images of whole-heart vertical cross section indicate increased wall thickness of right ventricles in MCT- and CH-PAH rats (Fig. 14). Also, the ratio of right

ventricle (RV) weight over the left ventricle and septum (RV/LV+S) increased significantly in MCT and CH rats (Fig. 14E, *** $P < 0.001$, ** $P < 0.01$). aling with from the right ventricular hypertrophy, the body weight increase was significantly attenuated in MCT and CH rats compared with saline injected and normoxia rats (Fig. 15A, ** $P < 0.01$). In CH rats, the hematocrit was consistently higher than that of normoxia rats (63.52 ± 1.57 % and 49.08 ± 0.94 %, respectively) (Fig. 15B, *** $P < 0.001$).

Finally, the TXA_2/L-NAME contraction was analyzed in the S(+) PAs in the PAH model rats. The TXA_2/L-NAME contraction normalized to 80K contraction was markedly in MCT rats when compared with the endothelium-denuded S(+) PAs from saline injected rats (Fig. 16). Likewise, TXA_2/L-NAME contraction in S(+) PAs from CH rats almost disappeared (Fig. 17).

Table 1. Nucleic acid sequences of the primers used for RT-PCR

Protein	Primer	Sequence (5' to 3')	Size (bp)
nNOS	Forward	GAACACGTTTGGGGTTCAGC	125
	Reverse	CTGAGATGATCACGGGAGGC	
iNOS	Forward	CCAGGTGCTATTCCCAGCC	518
	Reverse	GACCACTGAATCCTGCCGAT	
eNOS	Forward	TGTGACCCTCACCGATACAA	341
	Reverse	CTGGCCTTCTGCTCATTTTC	
GAPDH	Forward	GCCAAGGCTGTGGGCAAGGT	268
	Reverse	GAGCAATGCCAGCCCCAGCA	
PECAM-1	Forward	GGGAGGTATCGAATGGGCCAG	561
	Reverse	AGAACTCCTGCACAGTGACG	

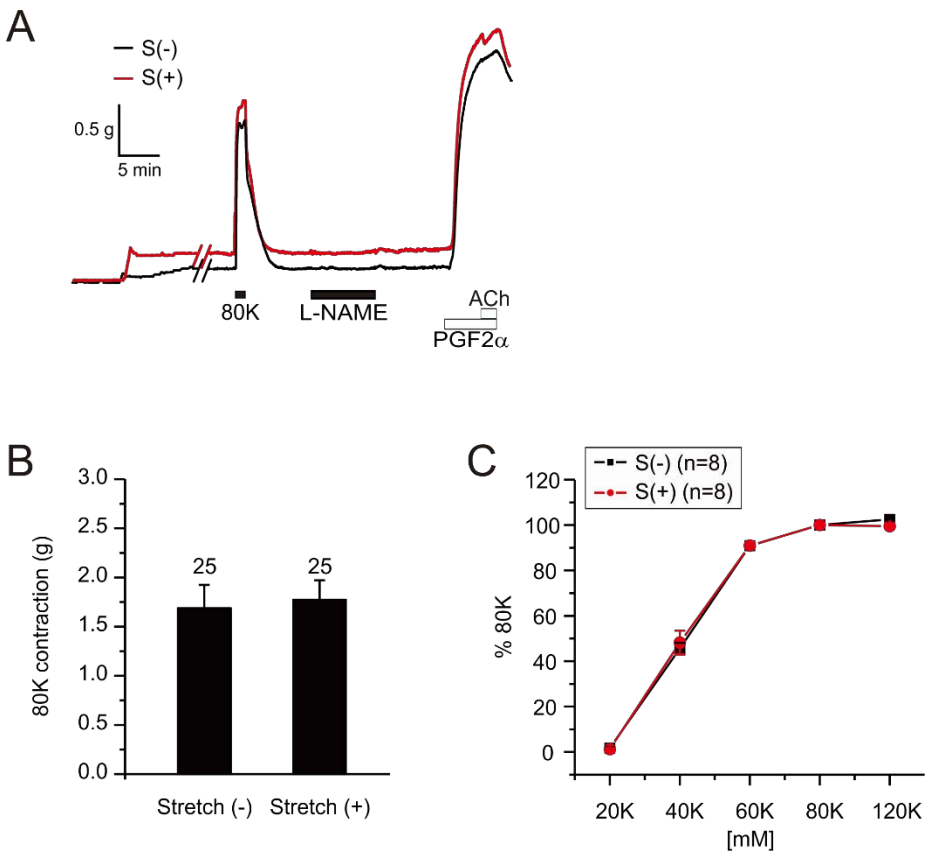

Figure 2. No different responses to contraction in S(−) and S(+) endothelium−deprived rat PA.

(A) Representative traces of PA tone recording. 80K contraction was confirmed initially, and the lack of ACh−induced relaxation was also confirmed at the end of each experiment. Neither S(−) PA nor S(+) PA showed response to L−NAME (100 μM) only. (B) Bar graph of absolute value for 80K contraction in S(−) and S(+) PAs (C) No difference of sensitivity to a series of raised $[K^+]_{ext}$ between S(−) PA and S(+) PA (n=8, respectively).

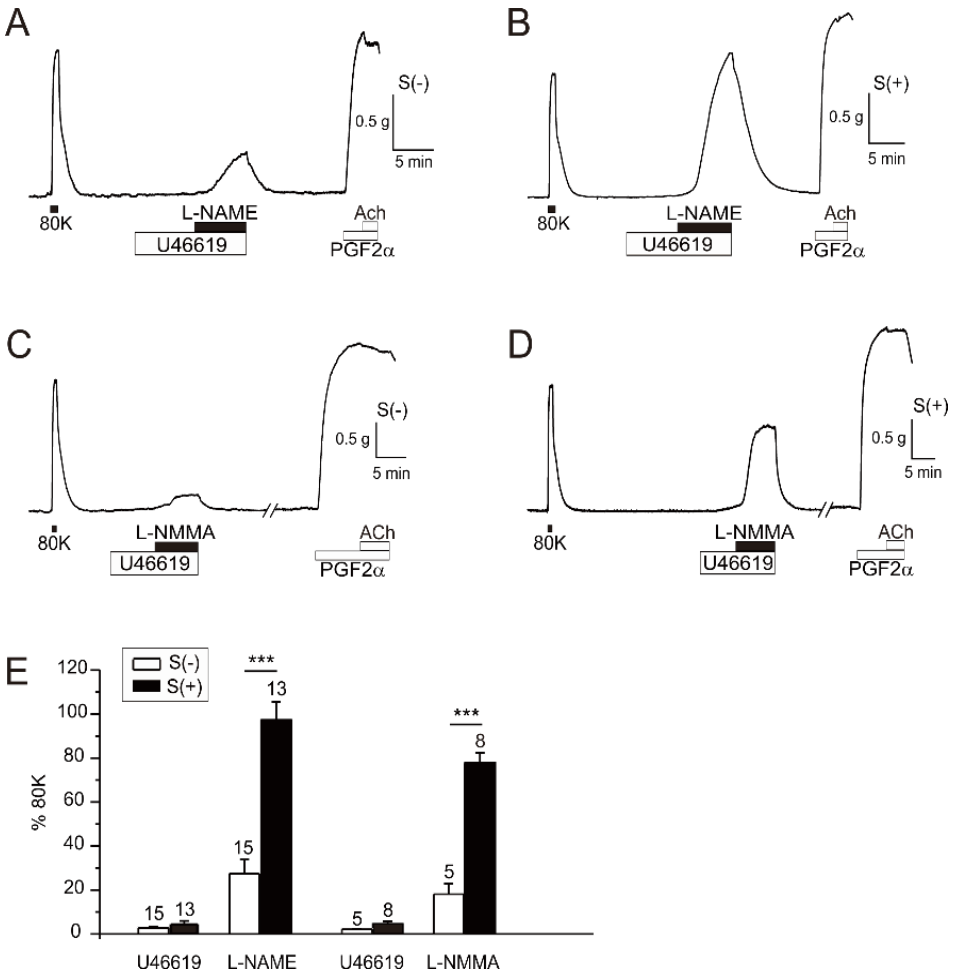

Figure 3. Augmentation of TXA_2/L−NAME contraction by higher basal stretch in endothelium−deprived rat PA.

(A) A representative trace of feeble TXA_2/L−NAME contraction in S(−) PA. (B) A representative trace of robust TXA_2/L−NAME contraction in S(+) PA. (C) A representative trace of weak contraction by TXA_2/L−NMMA (100 μM) in S(−) PA. (D) A representative trace of strong contraction by TXA_2/L−NMMA (100 μM) in S(+) PA (E) Summary of TXA_2/L−NAME and TXA_2/L−NMMA contraction in PAs. The level of tone was normalized to the 80K contraction in each vessel. Low (S(−)), and high (S(+)) levels of basal stretch for PA data are

summarized with white (n=15 and 5) and black (n=13 and 8) bars, respectively. There are significant differences in response to L-NAME and L-NMMA between S(-) and S(+) PAs (*** $P < 0.001$). The numbers of tested arteries are indicated above each bar.

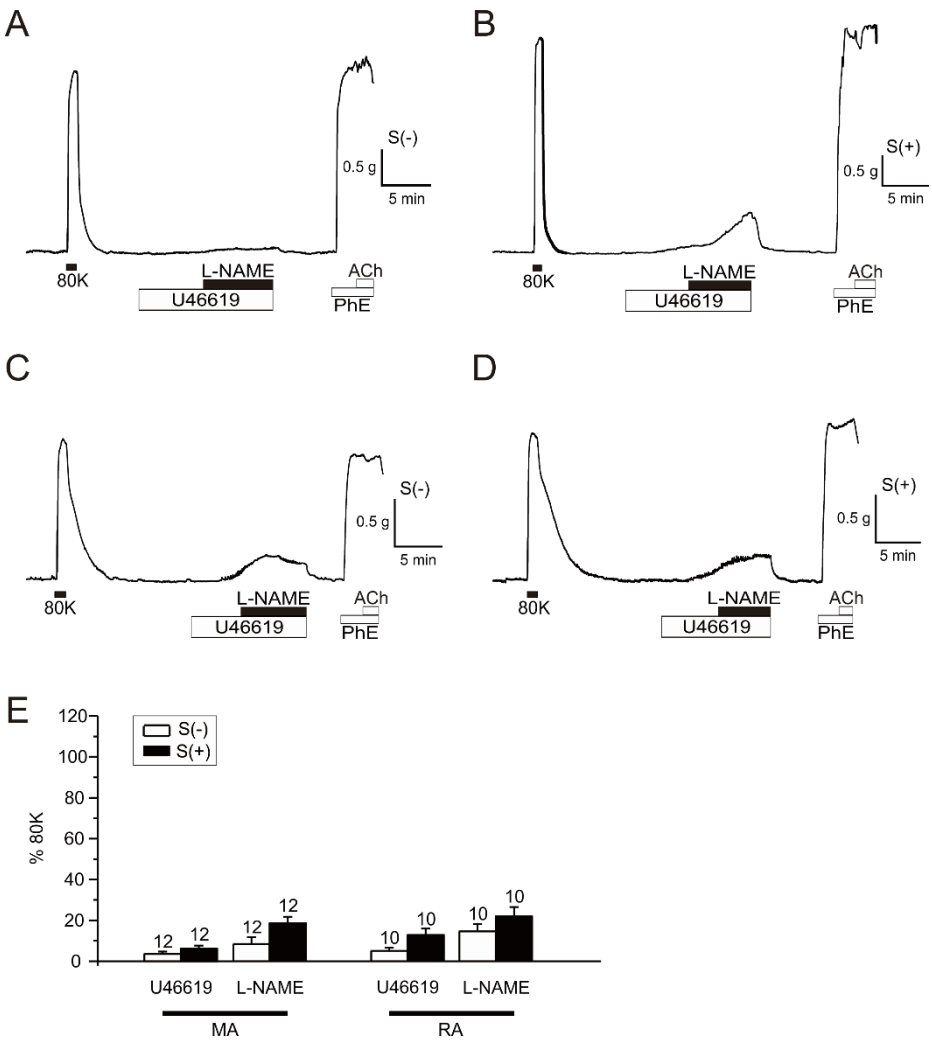

Figure 4. Minute effects of pretone stretch on TXA_2/L−NAME induced contraction in MAs and RAs

(A, B) Representative traces of weak TXA_2/L−NAME contraction in both S(−) and S(+) MAs. (C, D) Representative traces of feeble TXA_2/L−NAME contraction in both S(−) and S(+) RAs. (E) Summary of TXA_2/L−NAME contraction in MAs (n=12, respectively) and RAs (n=10, respectively).

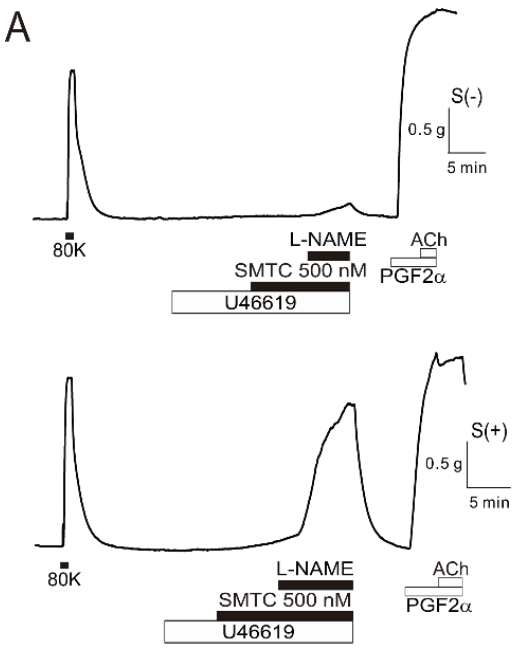
A
S(-)
0.5 g
5 min
80K
L-NAME
SMTC 500 nM
U46619
ACh
PGF2α
S(+)
0.5 g
5 min
80K
L-NAME
SMTC 500 nM
U46619
ACh
PGF2α

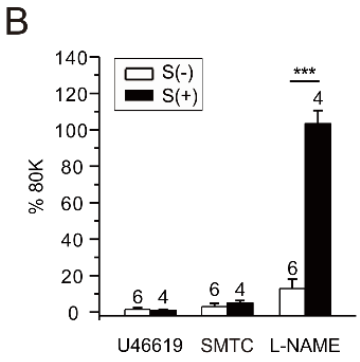
B
% 80K
S(-)
S(+)
***
U46619
SMTC
L-NAME

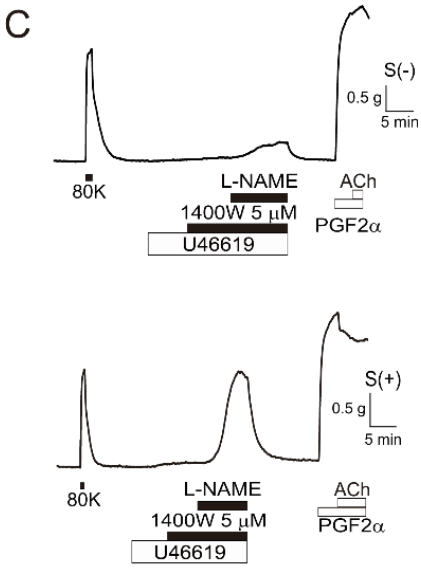
C
S(-)
0.5 g
5 min
80K
L-NAME
1400W 5 μM
U46619
ACh
PGF2α
S(+)
0.5 g
5 min
80K
L-NAME
1400W 5 μM
U46619
ACh
PGF2α

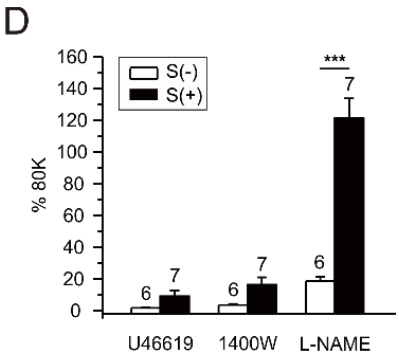
D
% 80K
S(-)
S(+)
***
U46619
1400W
L-NAME

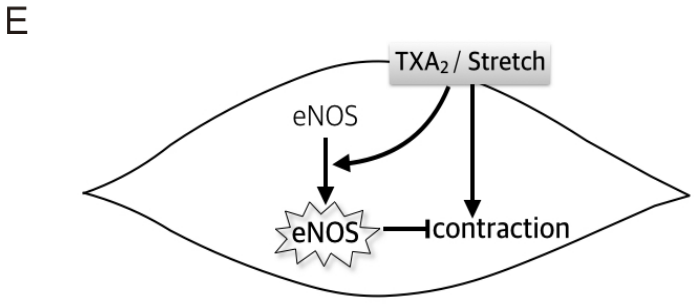
E
TXA2 / Stretch
eNOS
eNOS
contraction

Figure 5. Pharmacological evidences indicating the role of eNOS in TXA_2/L−NAME contraction of S(+) PAs

(A, C) Representative traces of PA tone showing the lack of effects by nNOS inhibitor (500 nM, SMTC, A) and iNOS inhibitor (5 μM 1400W, C) on U46619−pretreated PA. In contrast, large amplitude of TXA_2/L−NAME was consistently observed irrespective of SMTC and 1400W treatment. (B, D) Summary of the changes in PA tone normalized to the 80K contraction in each experiment. (B. S(−) n=6, S(+) n=8, D. S(−) n=6, S(+) n=7) *** $P < 0.001$. (E) Hypothetical model of eNOS expression in PASMC and physiological implication of TXA_2/stretch−induced eNOS activation that antagonize the concomitant stimulation of contractile signals.

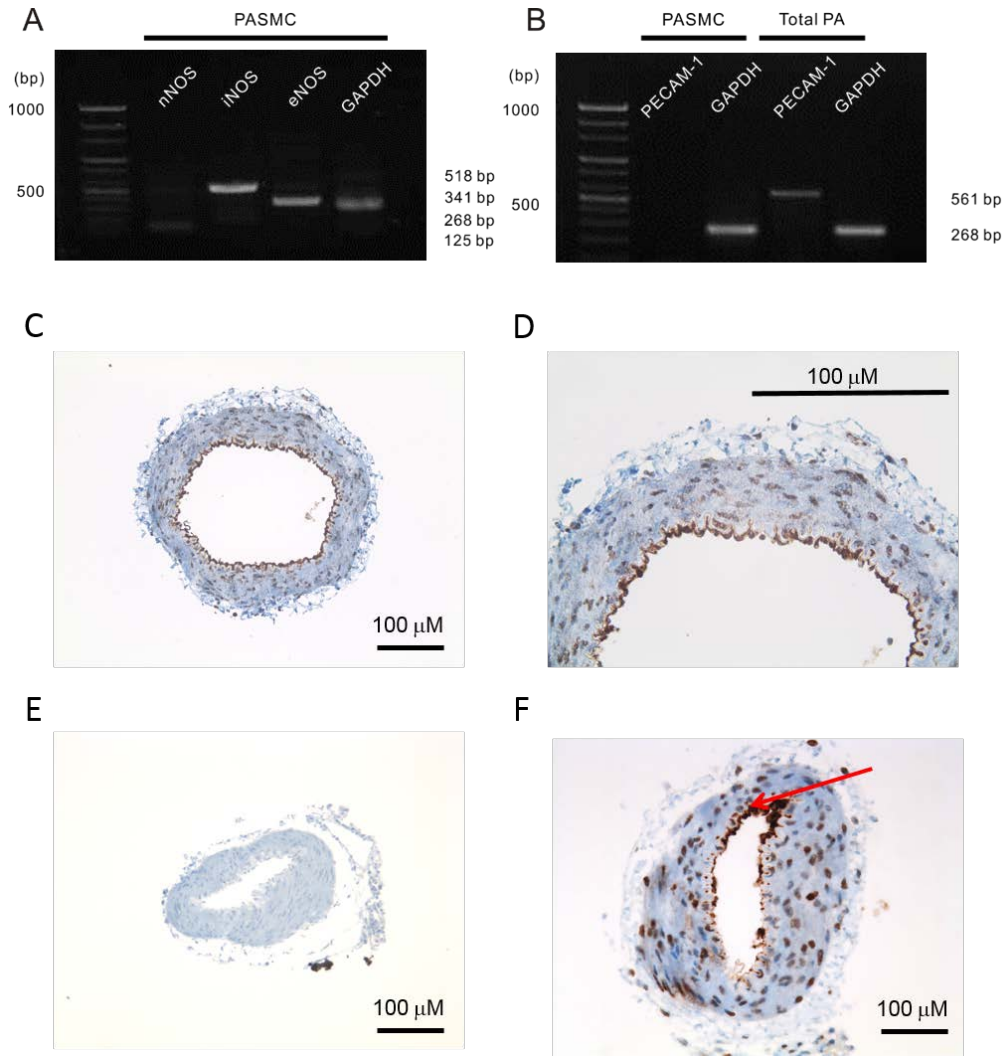
A
PASMC
(bp)
1000
500
nNOS
iNOS
eNOS
GAPDH
518 bp
341 bp
268 bp
125 bp
B
PASMC
Total PA
(bp)
1000
500
PECAM-1
GAPDH
PECAM-1
GAPDH
561 bp
268 bp
C
100 μM
D
100 μM
E
100 μM
F
100 μM

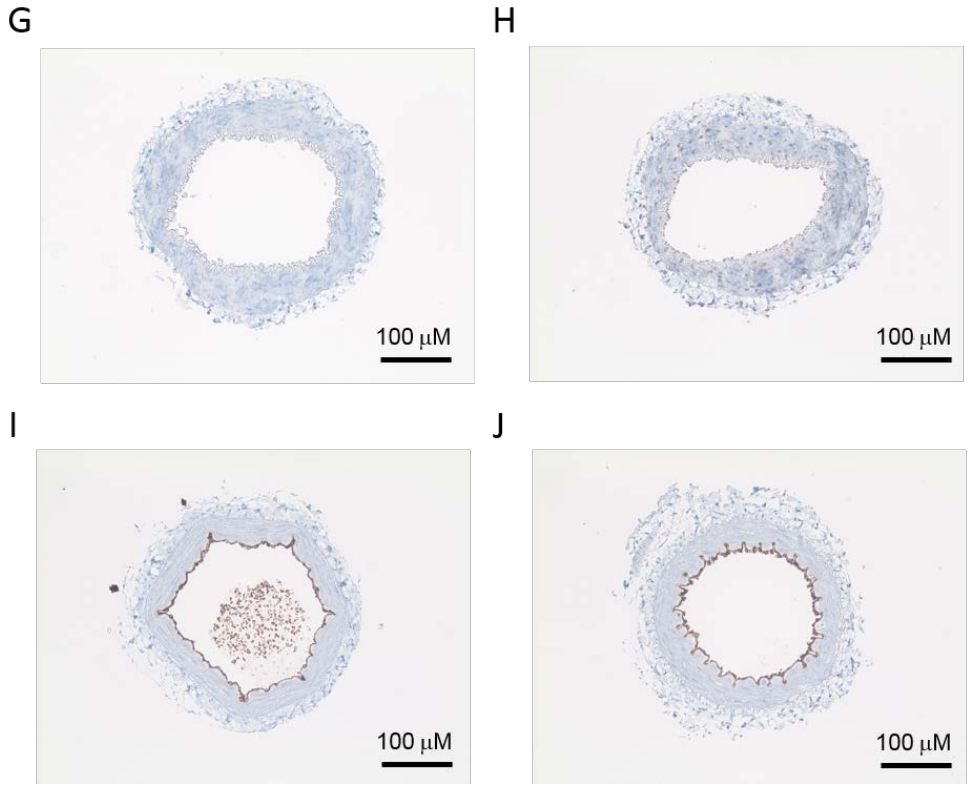

Figure 6. Verification of eNOS expression in PASMCs

(A) Expression of eNOS mRNA in isolated PASMCs. (B) Absence of mRNA for PECAM-1, an endothelium specific marker protein, in the isolated PASMC sample in contrast to the positive PECAM-1 signal in total PA sample. Representative images of the immunohistochemistry assays for eNOS in PA (C), expended eNOS in PA (D), negative control of eNOS in PA (E), eNOS in PA, red arrow indicated unremoved endothelium (F), nNOS in PA (G), iNOS in PA (H),eNOS in MA (I), and eNOS in RA (J), respectively. Positive signal of eNOS is commonly prominent in the endothelial layers of PA, MA and RA (C, F & G). Note the diffusive eNOS positive signal in the medial layer of PA (C).

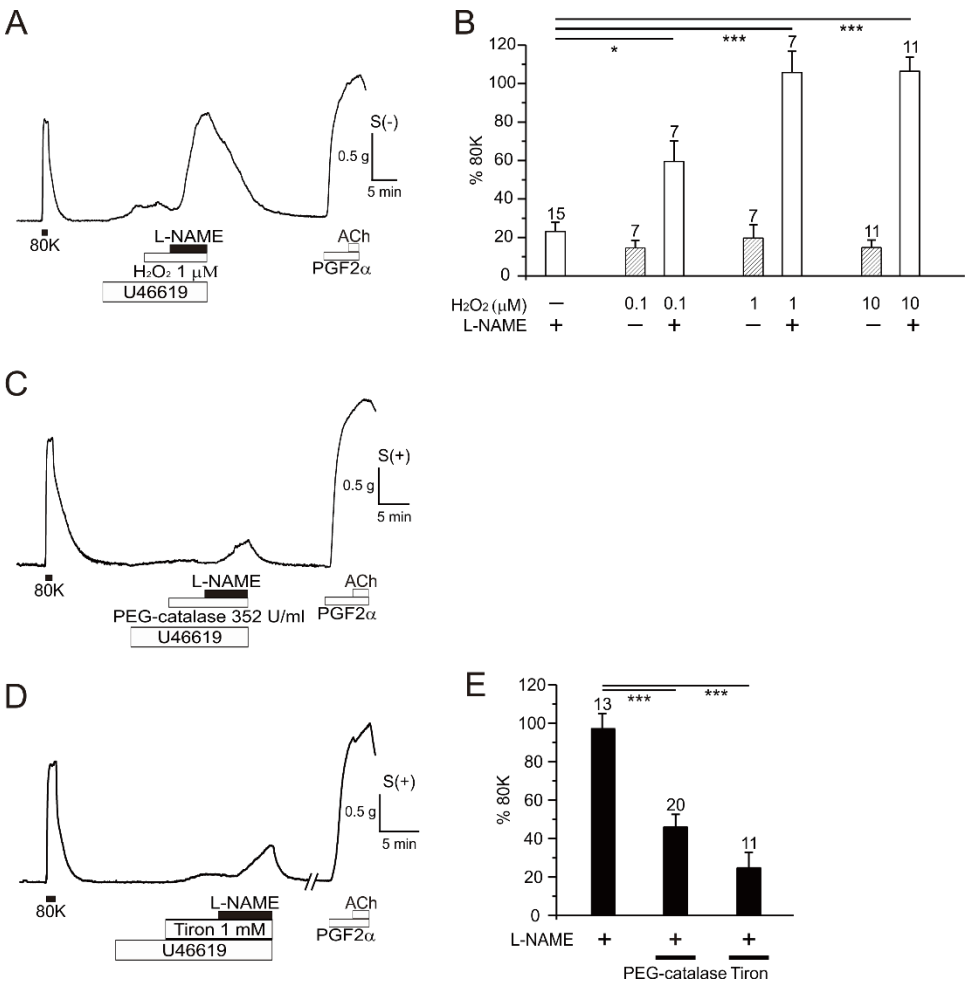

Figure 7. Critical role of H_2O_2 in TXA_2/L−NAME of PAs

(A) A representative trace showing significant TXA_2/L−NAME in S(−) PA treated with 1 μM H_2O_2. (B) Summary of 0.1 μM (n=7), 1 μM (n=7), and 10 μM (n=11) H_2O_2 pretreatment on TXA_2/L−NAME in S(−) PAs. Number of tested PAs is shown above each bar. Hatched bars indicate normalized S(−) PA tones with H_2O_2 before applying L−NAME. (*, $P < 0.05$; ***, $P < 0.001$). (C, D) Contraction of L−NAME significantly diminished by ROS scavenger (Tiron and PEG−catalase) in S(+) PA. (E) Summary of the inhibitory effects of Tiron (n=11) and PEG−catalase (n=20) on TXA_2/L−NAME in S(+) PA *** $P < 0.001$. Numbers of tested arteries are indicated above each bar.

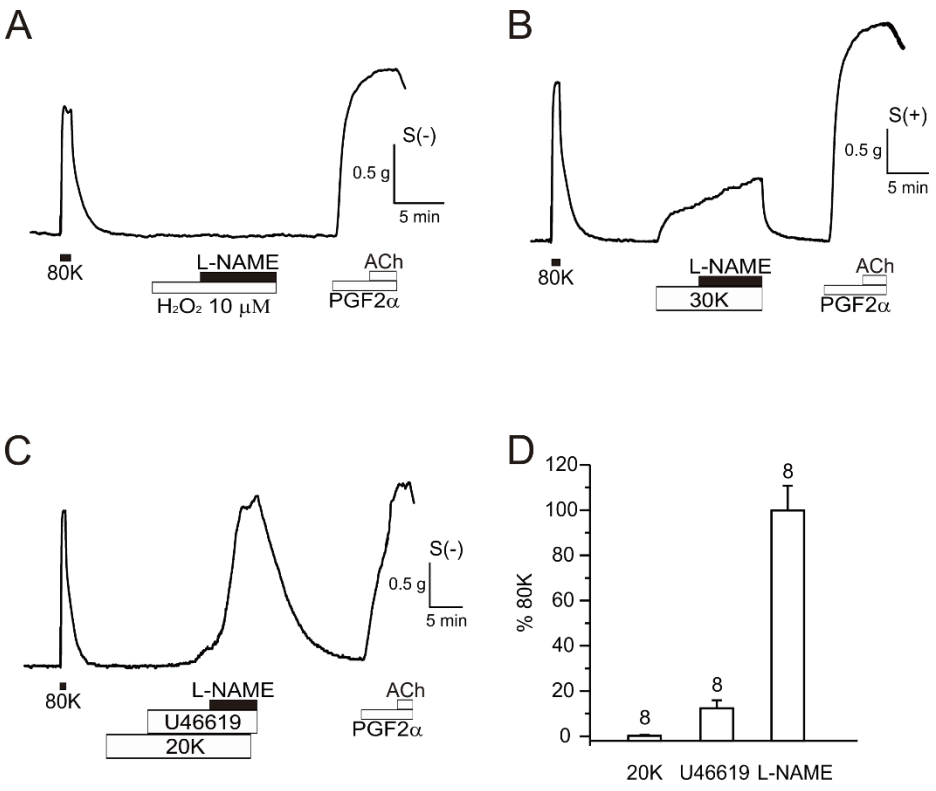

Figure 8. Requirement of pretone agent, U46619 in TXA_2/L-NAME of PAs

(A) A representative trace showing no response to L-NAME combined with 10 μM H_2O_2 without U46619 in S(-) PA. (B) A raw trace of L-NAME response in S(+) PA combined with partial contraction by 30 mM potassium solution (30K) as a pretone instead of U46619. (C) Contraction of L-NAME significantly increased by partial depolarization (20K) with U46619 in S(-) PA. (D) Summary of the partial depolarization effects of 20K mixed with U466619 in S(-) PA (n=8).

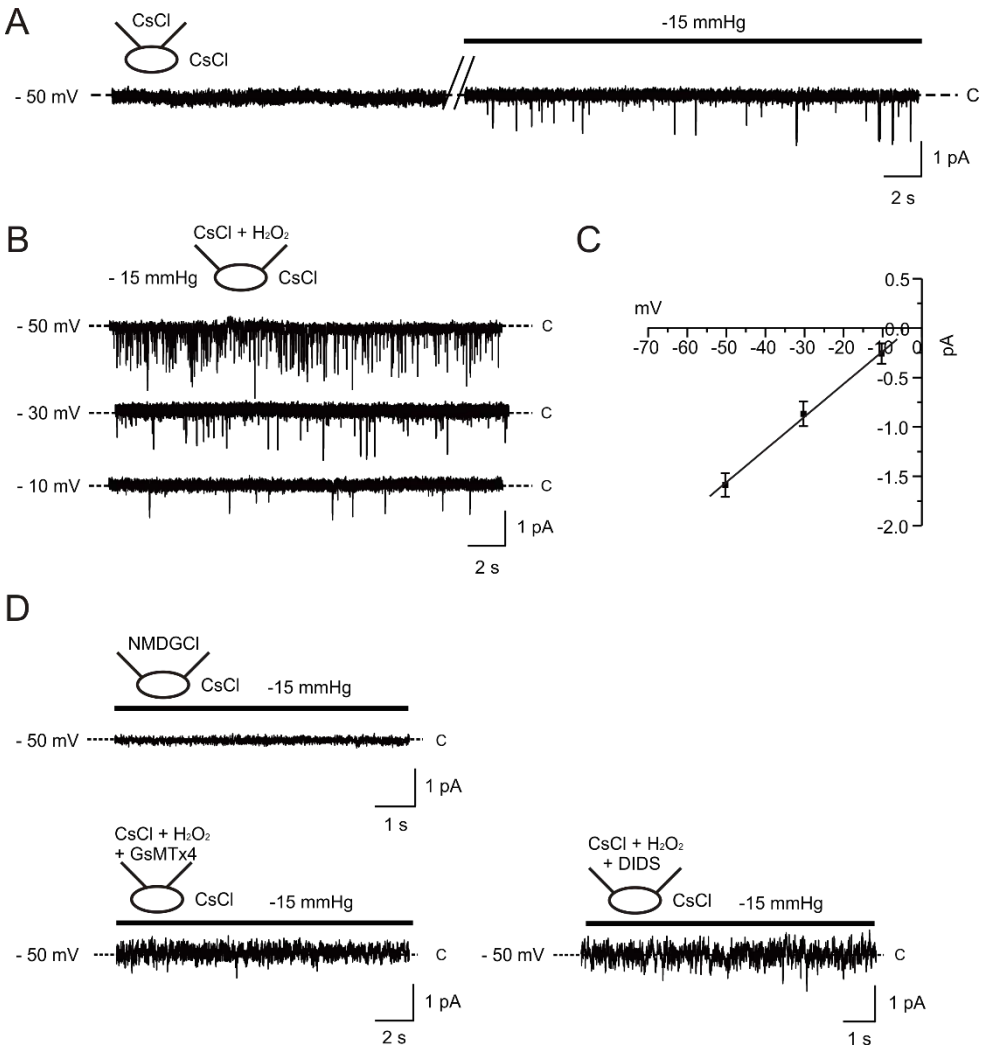

Figure 9. Stretch- and H_2O_2-induced cation channel activity

(A) A representative trace of SACs recorded in cell-attached patch clamp mode with CsCl pipette solution. Negative pressure (-15 mmHg) was applied through the patch pipette. The letters "C" represent closed state of channels. (B) (C) Unitary current to voltage relation of SAC. Slope conductance was obtained by liner fitting of I/V relation (33.1 ± 3.93 pS, n=14). (D)No such SAC activity was observed with 3 μM GsMTx4 (bottom).

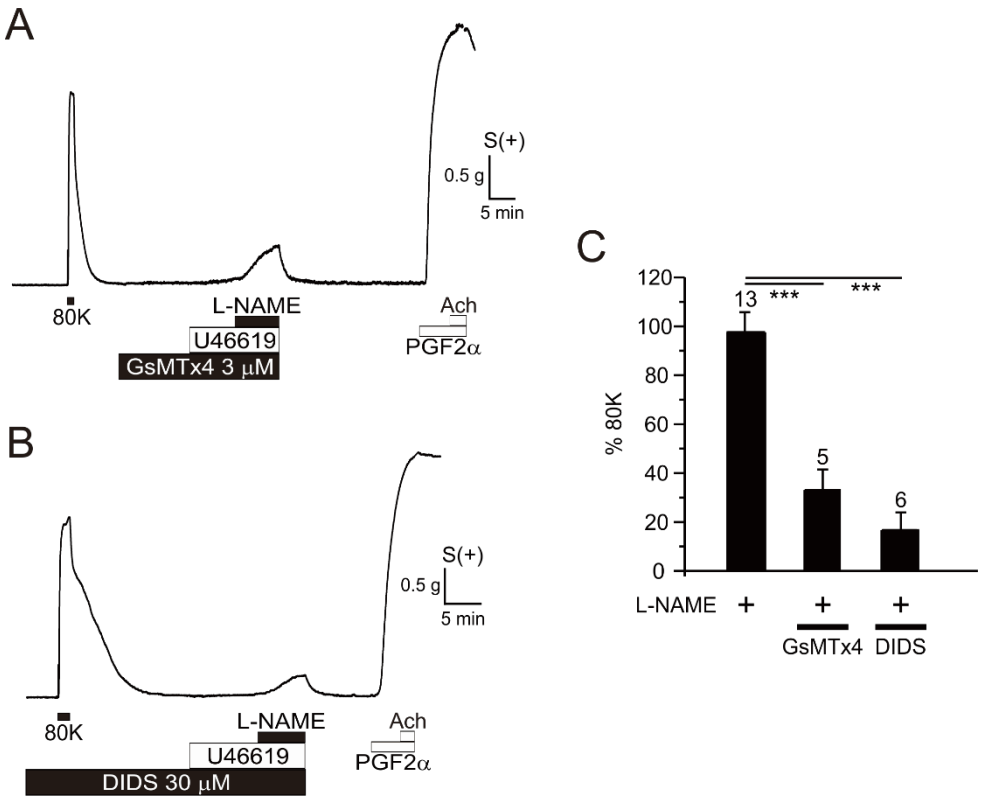

Figure 10. Inhibition of TXA_2/L-NAME contraction in S(+) PAs by stretch activated channels inhibitors

(A, B) Raw traces of inhibition TXA_2/L-NAME in S(+) PAs by pretreatment with 3 μM GsMTx4 (A) and 30 μM DIDS (B), SAC inhibitors. (C) Summary of the effects of SAC inhibitors on the TXA_2/L-NAME-contraction in S(+) PA (GsMTx4 n=5, DIDS n=6) *** $P < 0.001$

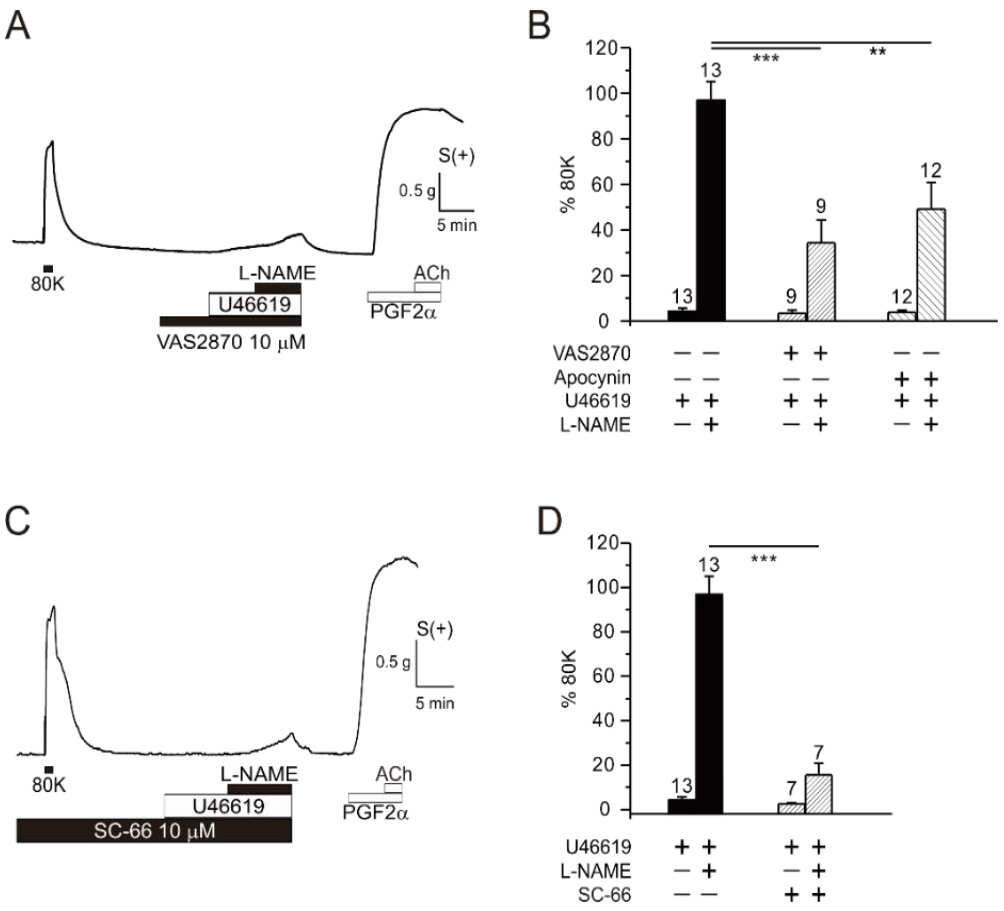

Figure 11. Effects of NOX and Akt signaling in eNOS activation mechanism of PAs.

(A) Decrease of TXA_2/L−NAME contraction in S(+) PAs by VAS2870 (B) Bar graph of significant NOX inhibitors effects, VAS2870 10 μM (n=9, *** $P < 0.001$) and Apocynin 100 μM (n=12, ** $P < 0.01$) (C) A representative trace of treatment of Akt inhibitor SC−66 10 μM in S(+) (D) Summary of SC−66 effect on TXA_2/L−NAME contraction in S(+) PAs (n=7, *** $P < 0.001$) Numbers of tested arteries are indicated above each bar.

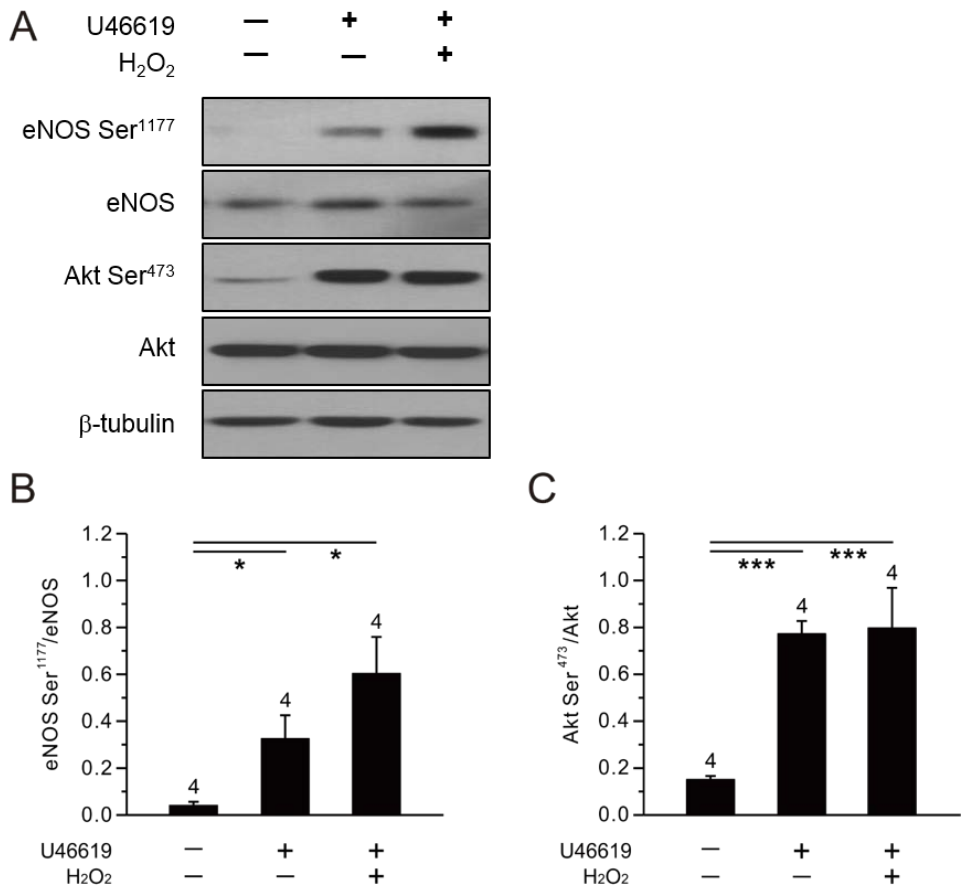

Figure 12. Immunoblot analysis of eNOS and Akt phosphorylation by U46619 and H_2O_2 in human PASMCs.

(A) Representative immunoblot images of eNOS and Akt, and their phosphorylation in the human PAMSCs. (B) Average ratio of eNOS Ser^{1177}/eNOS in control, 5 nM U46619−, and U46619/ 10 μM H_2O_2− cotreated cells (n=4, respectively). *, $P < 0.05$ (C) Average ratio of Akt Ser^{473}/Akt in control, 5 nM U46619− and U46619/ 10 μM H_2O_2− cotreated cells (n=4, respectively). ***, $P < 0.001$.

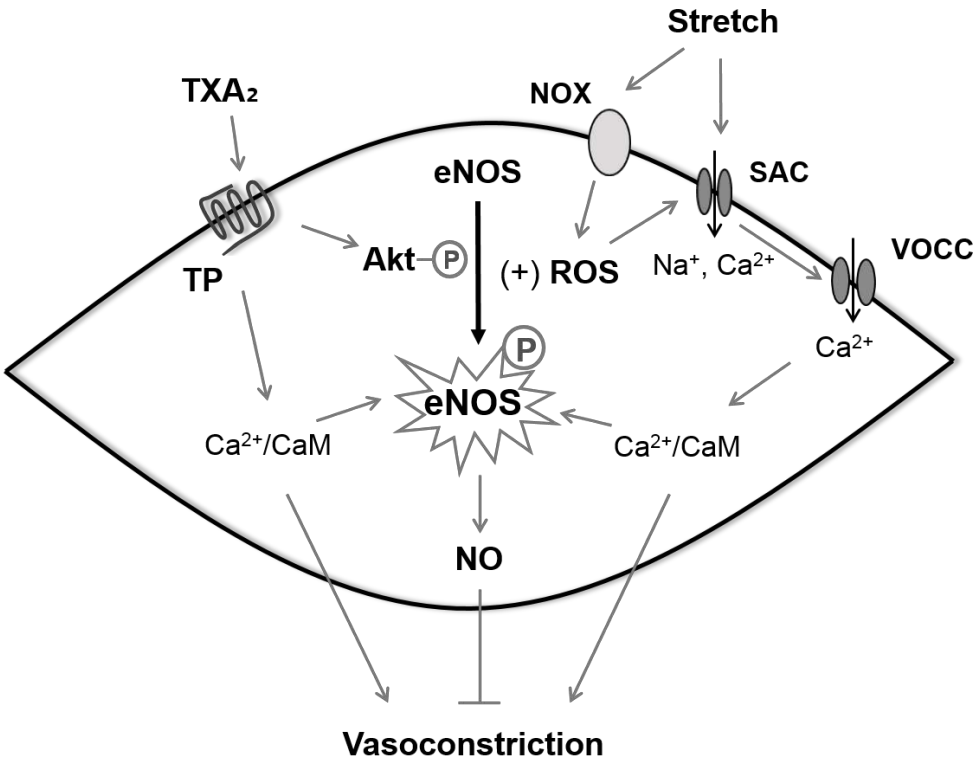

Figure 13. Schematic model of key steps regulating eNOS by mechanical stretch and thromboxane A_2 in PASMC.

Suggested signaling pathways affecting eNOS are depicted with arrows.

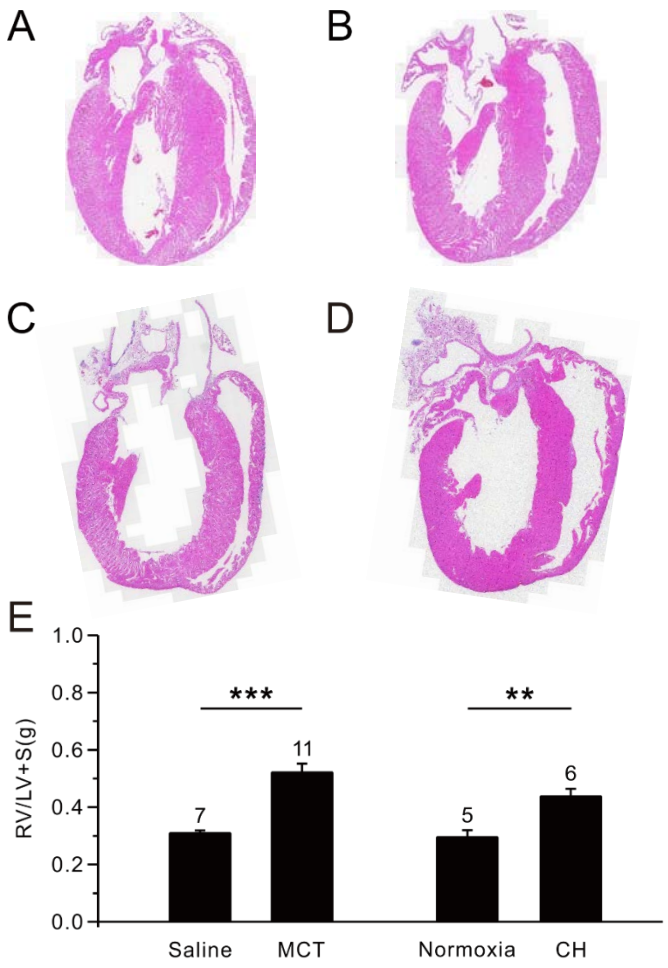

Figure 14. Right ventricle hypertrophy in MCT and CH rats.

H&E staining showed right ventricle wall thickening in MCT and CH rats. (A: saline, B: MCT, C: normoxia, D: CH). In MCT and CH rats, the ratio of right ventricle (RV) weight over the left ventricle and septum (RV/LV+S) was higher than saline and normoxia, ***, $P < 0.001$ (E).

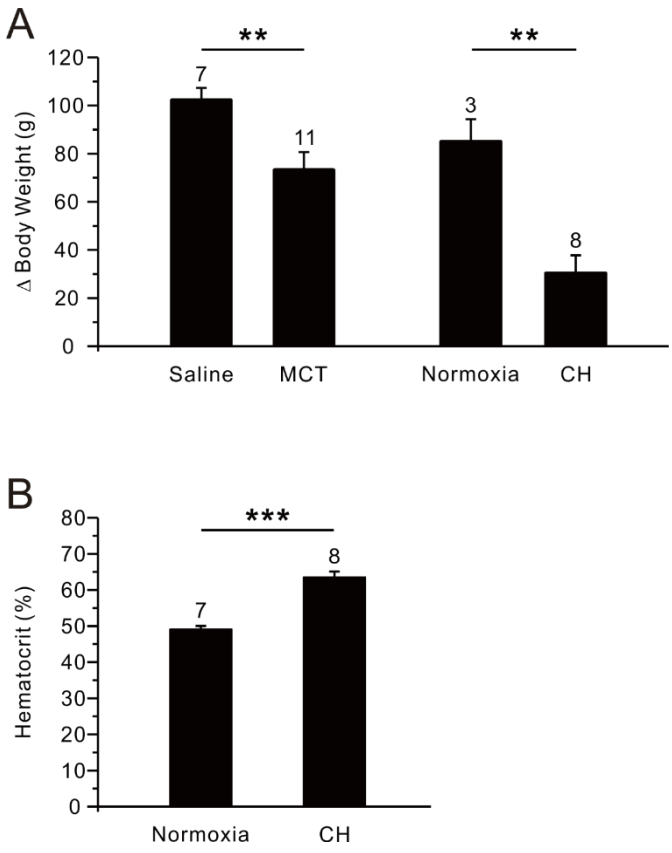

Figure 15. Showed body weight growth in MCT or CH rats, and increased hematocrit in CH rats.

(A) Body weight gain pattern was attenuated in MCT and CH rats, **, $P < 0.01$. (B) Hematocrit from CH rats significantly increased, ***, $P < 0.001$.

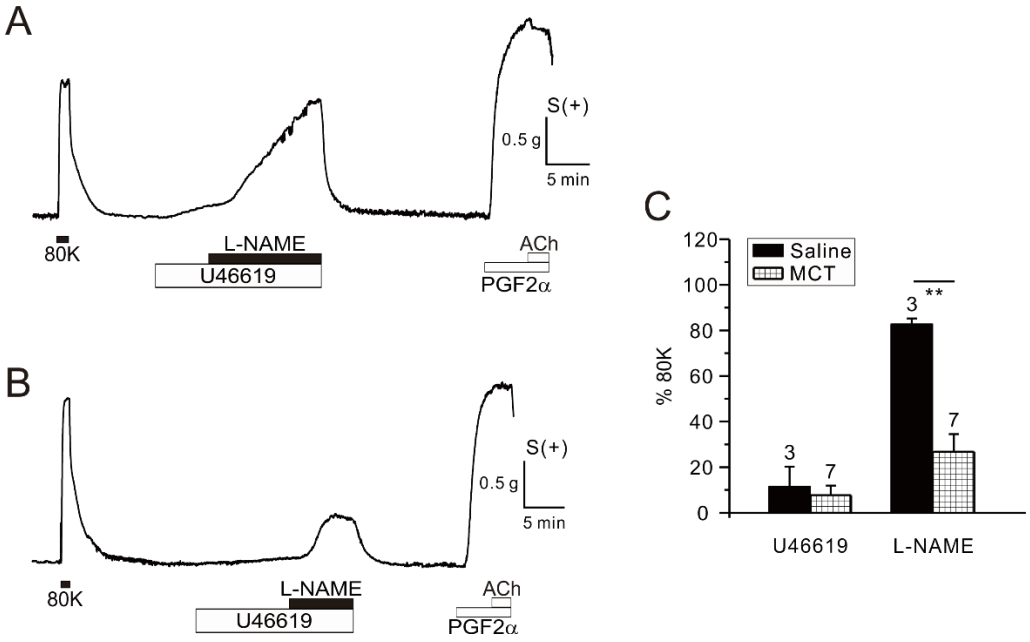

Figure 16. Decreased TXA_2/L−NAME contraction in S(+) PAs of MCT rats.

(A) A raw trace of large contraction by TXA_2/L−NAME in S(+) PA of saline injected rat. (B) A representative trace of weakened TXA_2/L−NAME contraction in S(+) PAS of MCT injected rats (C) Summarization of TXA_2/L−NAME contraction in S(+) PAs of saline (n=3) and MCT rats (n=7), **, $P < 0.01$.

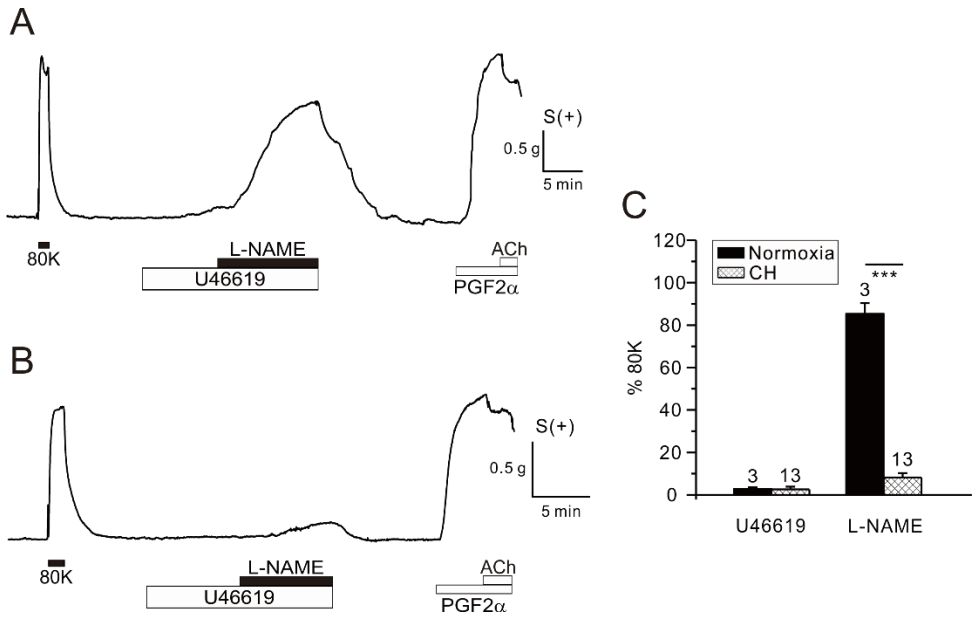

Figure 17. Decreased TXA_2/L-NAME contraction in S(+) PAs of CH rats.

(A) A representative trace of TXA_2/L-NAME contraction in S(+) PA of normoxia rat (B) A representative trace of decreased TXA_2/L-NAME contraction in S(+) PAs of CH rat model (C) Summarization of TXA_2/L-NAME contraction in S(+) PAs of normoxia (n=3) and CH rats (n=13), ***, $P < 0.001$.

DISCUSSION

The present study demonstrates the expression of eNOS in PASMCs. The eNOS expressed in PASMCs appears to be activated by a low level of TP stimulation, which is significantly enhanced when exposed to vascular wall stretch stress. The robust contraction of TXA_2/L-NAME observed in endothelium-deprived S(+) PAs suggests that muscular eNOS actually counterbalances the vasoconstricting signals induced by mechanical stretch and TP receptors stimulation in the pulmonary circulation. In S(+) PAs, NOX/H_2O_2-dependent signaling mechanisms mediated by mechanical stretch seem to underlie both eNOS phosphorylation pathways and the facilitation of SACs (Fig. 13).

The first question of the present study would be the reliability of the evidence for expression of eNOS in PASMCs. In addition to the consistent contractile response to the NOS inhibitor (L-NAME) in endothelium-denuded PAs, our study present three forms of evidence to support the conclusion. First, the expression of eNOS mRNA was validated in isolated PASMCs by RT-PCR. Second, eNOS protein expression were detected in the medial layer of PAs by immunohistochemistry. Third, the

expression of eNOS protein was also confirmed in the human PASMC cell line. In fact, the reports of eNOS expression in vascular smooth muscle layers is not unprecedented (Han et al., 2013). However, the present study newly shows eNOS expression in PASMCs and its role in PAs.

Mechanism underlying the activation of eNOS in PASMCs

It is generally accepted that eNOS is activated by Ca^{2+}/CaM-dependent signaling pathway. In S(+) PAs, the activation of SACs would depolarization, the treatment with U46619, i.e. TP stimulation, would increase $[Ca^{2+}]_c$ via signaling pathways such as PLC/IP_3-dependent Ca^{2+} release. It is suspected that the increase of $[Ca^{2+}]_c$ in S(+) PAs treated with U46619 would stimulate the muscle expressed eNOS as well as the contractile mechanisms.

In addition, phosphorylation of specific residue increases the sensitivity of eNOS activation under relatively low ranges of $[Ca^{2+}]_c$ (McMurry et al., 2011; Tran et al., 2009). The immunoblot assay of human PASMCs revealed that 5 nM U46619 alone induced weak phosphorylation of Ser^{1177}, which could be significantly augmented by combined treatment with H_2O_2 (Fig. 12A, B). The facilitating effect of H_2O_2 on eNOS phosphorylation

was consistent with the strong TXA_2/L−NAME contraction in H_2O_2−treated S(−) PAs (Fig. 7A, B).

In addition, the treatment with micromolar concentration of H_2O_2 mimicked S(+)condition and TXA_2/L−NAME contraction in S(+) PAs was inhibited by Tiron, catalase, and NOX inhibitors as well (Fig. 7, 11). On the basis of these results, I hypothesized that mechanical stress−induced ROS signaling (e.g., H_2O_2) could induce or facilitate eNOS phosphorylation founded on reports that mechanical stretch activates NOX in a variety of vessels including PAs (Frazziano et al., 2012; Mata−Greenwood et al., 2005).

U46619−induced phosphorylation of Ser^{1177} of eNOS was different from a previous study in which insulin−treated endothelium showed inhibition of Ser^{1177} phosphorylation by 400 nM U46619 treatment (Song et al., 2009). To the best of my knowledge, the present study is the first to demonstrate TP−mediated Ser^{1177} phosphorylation of eNOS. The opposite responses might be due to differences in signaling pathways between endothelium and smooth muscle cells.

According to previous studies, H_2O_2 could facilitate Akt−dependent signaling by inhibiting protein phosphatase, which

increases the activated form of Akt phosphorylation; Akt Ser^{473} (Barbosa et al., 2013). Akt Ser^{473} phosphorylation is reported to induce eNOS Ser^{1177} phosphorylation in cardiovascular cells (Dossumbekova et al., 2008; Zhou et al., 2013). Consistently, treatment with an Akt inhibitor also attenuated the contractile response to TXA_2/L-NAME in S(+) PAs (Fig. 11C, D). In the present study, however, treatment with 5 nM U46619 alone could induce Ser^{473} phosphorylation of Akt (Fig. 12A, C). The additive effect of H_2O_2 on Ser^{1177} phosphorylation might imply another facilitating mechanism for eNOS activation. Also, I could not exclude the possibility that U46619 treatment induces ROS generation in PASMCs.

Role of SACs in the TXA_2/L-NAME contraction of PAs

The absence of TXA_2/L-NAME contraction in PEG-catalase- or Tiron-treated S(+) PAs suggested that not only Akt/eNOS activation but also contractile signals were stimulated by H_2O_2-dependent mechanisms (Fig. 7C-E). Interestingly, I provided electrophysiological evidence of H_2O_2-dependent SAC activation in rat PASMCs (Fig. 9B, C). Because the suppression of TXA_2/L-NAME in S(+) PAs by GsMTx4 and DIDS indicates the critical role of SACs and membrane depolarization in the

recruitment of eNOS (Fig. 9D, 10A–C).

Our group had reported that SACs isolated in rabbit PASMCs were recorded by electrophysiological methods before (Park et al., 2003; Park et al., 2006). However, in rat PASMCs, reliable recording of SACs was not possible in our hands. In fact, only once, Ducret group demonstrated the single-channel activities of SACs in rats (Ducret et al., 2010). Here, I newly found that addition of micromolar concentrations of H_2O_2 in the c-a patch pipette solution significantly facilitated the probability of SAC recordings (Fig. 9A, B). Intrinsic production of ROS and H_2O_2 might specifically underlie the physiological roles of SACs in rat PA contractility. In addition to the effect of U46619, a partial depolarization by SAC activation would increase the Ca^{2+}-influx via L-type Ca^{2+} channels. Along with the effects of H_2O_2 on the phosphorylation of eNOS, the expected increase in $[Ca^{2+}]_c$ may facilitate the Ca^{2+}-dependent eNOS activation.

SACs in vascular smooth muscle are a major sensor/effector component in the contractile response of resistance arteries to increasing wall tension, called the myogenic response. It is reported that normal PAs do not show the myogenic contractile responses (Belik, 1994; Naik et al., 2005). The lack of a

myogenic response in PAs might be due to the relaxing influence of intrinsic muscular eNOS that is activated by mechanical stress.

Despite the critical roles of SACs in the TXA_2/L−NAME contraction, it should be noted that TP−dependent signaling is indispensable because the H_2O_2 treatment alone or the partial depolarization by 30 mM K^+ itself could not allow a significant contraction by L−NAME only even in S(+) PAs (Fig. 8A, B). Furthermore, the requirement of membrane depolarization combined with TP receptor stimulation for TXA_2/L−NAME contraction was suggested from the effect of 20 mM K^+−induced partial depolarization on the TXA_2/L−NAME contraction in S(+) PAs (Fig. 8C, D).

Physiological and pathophysiological implications

According to the present study, the contractile responses of PASMCs to TXA_2 and basal stretch seem to be effectively compromised by concomitant activation of muscular eNOS. Despite strong expression of eNOS in the endothelial layer, only a diffusive supply of NO from intima might be insufficient to relax the feeding PAs with multiple layers of smooth muscle cells. Muscular eNOS may provide an automatic counterbalance against contraction by paracrine agonists and neurotransmitters released

from adventitia (Fig. 1).

Pulmonary arterial hypertension (PAH) is a fatal progressive disease characterized by increased pulmonary vascular pressure and pulmonary vascular remodeling leading to an increase in pulmonary vascular resistance and right ventricle failure (Gomez-Arroyo et al., 2012). The most commonly used animal models of PAH are the injection of monocrotaline (MCT) and the chronic hypoxia (CH) exposure to investigate human PAH over a long period of time comparing with each other (Pak et al., 2010). The MCT is toxic pyrrolizidine alkaloid which affected endothelial and interstitial cells initially damaging the pulmonary small arteries and capillaries (Alexandru and Bogdan, 2001; Dumitrascu et al., 2008; Huxtable, 1990). Previous studies focused on pulmonary vascular function such as endothelium dysfunction, response of vasoconstrictors or vasodilators in animal models of PAH with variable results (Barman, 2007; Mam et al., 2010). However, the specificity of the effects of PAH on the pulmonary circulation compared with other systemic vascular systems had not been clearly established still. Moreover, the molecular mechanism of PAH is not known yet, but it is reported that vasodilators derived from endothelium such as NO or

prostacyclin declined because of endothelium dysfunction (Budhiraja et al., 2004). Also, there was a stimulation of the synthesis of vasoconstrictors and many pathways were involved in the abnormal proliferation and severe contraction of the smooth muscle cells of PAs causing smooth muscle hypertrophy in PAH patients. Consequently TXA_2/L-NAME contraction disappeared in MCT and CH S(+)PAs (Fig. 16B-C, 17B-C), this study suggests that loss of muscular eNOS preventing excessive contraction could contribute to develop PAH. Through a study such as above, muscular eNOS would be one of basic foundations to access therapeutic approaches.

Limitations of the study

A critical limitation of the present study is the lack of direct evidence from *in vivo* experiments proving the physiological significance of muscular eNOS. An *in situ* study of artificially ventilated and perfused lungs from rats might provide an integrative understanding of the role of muscular eNOS. However, because of the presence of intact endothelium in the whole organ and animal studies, it would be very difficult to distinguish between the contributions of muscular and endothelial eNOS. Further investigation of the changes in functional eNOS

expression in chronic lung diseases (e.g., pulmonary hypertension and chronic hypoxia) along with ion channel currents might provide intriguing knowledge to understand the pathophysiological mechanisms (Yoo and Kim, 2013).

Conclusion

Taken together, I propose the expression and functional role of eNOS in PASMCs in response to wall stretch and TXA_2 for the first time. The present results imply that TP stimulation and stretch-induced H_2O_2 effectively facilitate muscular eNOS via phosphorylation. I cautiously suggest that the relaxing influences might contribute to the active lowering of pulmonary resistance, which is important for coping with the large fluctuations in venous return to the pulmonary vascular system.

REFERENCES

1. Alexandru B, Bogdan MA. Monocrotaline induce pulmonary hypertension in animal models. *Pneumologia*. 2001;50(2):85-9.

2. Baek EB, Kim SJ. Mechanisms of myogenic response: Ca^{2+}-dependent and -independent signaling. *J Smooth Muscle Res*. 2011;47(2):55-65.

3. Barbera JA, Peinado VI, Santos S, Ramirez J, Roca J, Rodriguez-Roisin R. Reduced expression of endothelial nitric oxide synthase in pulmonary arteries of smokers. *Am J of Respir Crit Care Med*. 2001;164(4):709-13.

4. Barbosa VA, Luciano TF, Marques SO, Vitto MF, Souza DR, Silva LA, et al. Acute exercise induce endothelial nitric oxide synthase phosphorylation via Akt and AMP-activated protein kinase in aorta of rats: Role of reactive oxygen species. *Int J Cardiol*. 2013;167(6):2983-8.

5. Barman SA. Vasoconstrictor effect of endothelin-1 on hypertensive pulmonary arterial smooth muscle involves Rho-kinase and protein kinase C. *Am J Physiol Lung Cell Mol Physiol*. 2007;293(2):L472-9.

6. Belik J. Myogenic response in large pulmonary arteries and its ontogenesis. *Pediatr Res*. 1994;36(1 Pt 1):34-40.

7. Bialecki RA, Kulik TJ, Colucci WS. Stretching increases calcium influx and efflux in cultured pulmonary arterial smooth muscle cells. *Am J Physiol*. 1992;263(5 Pt 1):L602-6.

8. Birukov KG. Cyclic stretch, reactive oxygen species, and vascular remodeling. *Antioxid Redox Signal*. 2009;11(7):1651-67.

9. Bowman CL, Gottlieb PA, Suchyna TM, Murphy YK, Sachs F. Mechanosensitive ion channels and the peptide inhibitor GsMTx-4: history, properties, mechanisms and pharmacology. *Toxicon*. 2007;49(2):249-70.

10. Breyer RM, Bagdassarian CK, Myers SA, Breyer MD. Prostanoid receptors: subtypes and signaling. *Annu Rev Pharmacol Toxicol*. 2001;41:661-90.

11. Buchwalow IB, Cacanyiova S, Neumann J, Samoilova VE, Boecker W, Kristek F. The role of arterial smooth muscle in vasorelaxation. *Biochem Biophys Res Commun*. 2008;377(2):504-7.

12. Buchwalow IB, Podzuweit T, Bocker W, Samoilova VE, Thomas S, Wellner M, et al. Vascular smooth muscle and nitric oxide synthase. *FASEB J*. 2002;16(6):500-8.

13. Budhiraja R, Tuder RM, Hassoun PM. Endothelial dysfunction in pulmonary hypertension. *Circulation*. 2004;109(2):159-65.

14. Cacanyiova S, Dovinova I, Kristek F. The role of oxidative stress in acetylcholine-induced relaxation of endothelium-denuded arteries. *J Physiol Pharmacol*. 2013;64(2):241-7.

15. Cahill E, Rowan SC, Sands M, Banahan M, Ryan D, Howell K, et al. The pathophysiological basis of chronic hypoxic pulmonary hypertension in the mouse: vasoconstrictor and structural mechanisms contribute equally. *Exp Physiol*. 2012;97(6):796-806.

16. Chen R, Kim O, Yang J, Sato K, Eisenmann KM, McCarthy J, et al. Regulation of Akt/PKB activation by tyrosine phosphorylation. J Biol Chem. 2001;276(34):31858-62.

17. Cogolludo A, Moreno L, Bosca L, Tamargo J, Perez-Vizcaino F. Thromboxane A_2-induced inhibition of voltage-gated K^+ channels and pulmonary vasoconstriction: role of protein kinase

Czeta. *Circ Res*. 2003;93(7):656-63.

18. Cooper CJ, Landzberg MJ, Anderson TJ, Charbonneau F, Creager MA, Ganz P, et al. Role of nitric oxide in the local regulation of pulmonary vascular resistance in humans. *Circulation*. 1996;93(2):266-71.

19. Dick AS, Ivanovska J, Kantores C, Belcastro R, Keith Tanswell A, Jankov RP. Cyclic stretch stimulates nitric oxide synthase-1-dependent peroxynitrite formation by neonatal rat pulmonary artery smooth muscle. *Free Radic Biol Med*. 2013;61:310-9.

20. Dikalova AE, Gongora MC, Harrison DG, Lambeth JD, Dikalov S, Griendling KK. Upregulation of Nox1 in vascular smooth muscle leads to impaired endothelium-dependent relaxation via eNOS uncoupling. *Am J Physiol Heart Circ Physiol*. 2010;299(3):H673-9.

21. Dossumbekova A, Berdyshev EV, Gorshkova I, Shao Z, Li C, Long P, et al. Akt activates NOS3 and separately restores barrier integrity in H_2O_2-stressed human cardiac microvascular endothelium. *Am J Physiol Heart Circ Physiol*.

2008;295(6):H2417-26.

22. Ducret T, El Arrouchi J, Courtois A, Quignard JF, Marthan R, Savineau JP. Stretch-activated channels in pulmonary arterial smooth muscle cells from normoxic and chronically hypoxic rats. *Cell calcium*. 2010;48(5):251-9.

23. Dumitrascu R, Koebrich S, Dony E, Weissmann N, Savai R, Pullamsetti SS, et al. Characterization of a murine model of monocrotaline pyrrole-induced acute lung injury. *BMC Pulm Med*. 2008;8:25.

24. Earley S, Walker BR. Increased nitric oxide production following chronic hypoxia contributes to attenuated systemic vasoconstriction. *Am J Physiol Heart Circ Physiol.* 2003;284(5):H1655-61.

25. Evora PR, Evora PM, Celotto AC, Rodrigues AJ, Joviliano EE. Cardiovascular therapeutics targets on the NO-sGC-cGMP signaling pathway: a critical overview. *Curr Drug Targets*. 2012;13(9):1207-14.

26. Fleming I. Molecular mechanisms underlying the activation of eNOS. *Pflugers Archiv*. 2010;459(6):793-806.

27. Frazziano G, Champion HC, Pagano PJ. NADPH oxidase-derived ROS and the regulation of pulmonary vessel tone. *Am J Physiol Heart Circ Physiol*. 2012;302(11):H2166-77.

28. Furfine ES, Harmon MF, Paith JE, Knowles RG, Salter M, Kiff RJ, et al. Potent and selective inhibition of human nitric oxide synthases. Selective inhibition of neuronal nitric oxide synthase by S-methyl-L-thiocitrulline and S-ethyl-L-thiocitrulline. *J Biol Chem*. 1994;269(43):26677-83.

29. Garvey EP, Oplinger JA, Furfine ES, Kiff RJ, Laszlo F, Whittle BJ, et al. 1400W is a slow, tight binding, and highly selective inhibitor of inducible nitric-oxide synthase in vitro and in vivo. *J Biol Chem*. 1997;272(8):4959-63.

30. Gomez-Arroyo JG, Farkas L, Alhussaini AA, Farkas D, Kraskauskas D, Voelkel NF, et al. The monocrotaline model of pulmonary hypertension in perspective. *Am J Physiol Lung Cell Mol Physiol*. 2012;302(4):L363-9.

31. Han JA, Seo EY, Kim HJ, Park SJ, Yoo HY, Kim JY, et al. Hypoxia-augmented constriction of deep femoral artery mediated by inhibition of eNOS in smooth muscle. *Am J Physiol*

Cell Physiol. 2013;304(1):C78-88.

32. Hill MA, Davis MJ, Meininger GA, Potocnik SJ, Murphy TV. Arteriolar myogenic signalling mechanisms: Implications for local vascular function. *Clin Hemorheol Microcirc*. 2006;34(1-2):67-79.

33. Huang JS, Ramamurthy SK, Lin X, Le Breton GC. Cell signalling through thromboxane A_2 receptors. *Cell signal*. 2004;16(5):521-33.

34. Huxtable RJ. Activation and pulmonary toxicity of pyrrolizidine alkaloids. *Pharmacol Ther.* 1990;47(3):371-89.

35. Kietadisorn R, Juni RP, Moens AL. Tackling endothelial dysfunction by modulating NOS uncoupling: new insights into its pathogenesis and therapeutic possibilities. *Am J Physiol Endocrinol Metab*. 2012;302(5):E481-95.

36. Kumar S, Sud N, Fonseca FV, Hou Y, Black SM. Shear stress stimulates nitric oxide signaling in pulmonary arterial endothelial cells via a reduction in catalase activity: role of protein kinase C delta. *Am J Physiol Lung Cell Mol Physiol*. 2010;298(1):L105-16.

37. Lee HA, Baek EB, Park KS, Jung HJ, Kim JI, Kim SJ, et al. Mechanosensitive nonselective cation channel facilitation by endothelin-1 is regulated by protein kinase C in arterial myocytes. *Cardiovas Res*. 2007;76(2):224-35.

38. Lumb AB, Nunn JF. Nunn's applied respiratory physiology. 6th ed. Elsevier. 2005; pp 92-104.

39. Mam V, Tanbe AF, Vitali SH, Arons E, Christou HA, Khalil RA. Impaired vasoconstriction and nitric oxide-mediated relaxation in pulmonary arteries of hypoxia- and monocrotaline-induced pulmonary hypertensive rats. *J Pharmacol Exp Ther*. 2010;332(2):455-62.

40. Mata-Greenwood E, Grobe A, Kumar S, Noskina Y, Black SM. Cyclic stretch increases VEGF expression in pulmonary arterial smooth muscle cells via TGF-beta1 and reactive oxygen species: a requirement for NAD(P)H oxidase. *Am J Physiol Lung Cell Mol Physiol*. 2005;289(2):L288-9.

41. Mathew R, Huang J, Gewitz MH. Pulmonary artery hypertension: caveolin-1 and eNOS interrelationship: a new perspective. *Cardiol Rev*. 2007;15(3):143-9.

42. McMurry JL, Chrestensen CA, Scott IM, Lee EW, Rahn AM, Johansen AM, et al. Rate, affinity and calcium dependence of nitric oxide synthase isoform binding to the primary physiological regulator calmodulin. *FEBS J*. 2011;278(24):4943-54.

43. Michel T, Vanhoutte PM. Cellular signaling and NO production. *Pflugers Archiv*. 2010;459(6):807-16.

44. Naik JS, Earley S, Resta TC, Walker BR. Pressure-induced smooth muscle cell depolarization in pulmonary arteries from control and chronically hypoxic rats does not cause myogenic vasoconstriction. *J Appl Physiol*. 2005;98(3):1119-24.

45. Nakayama K, Ueta K, Tanaka Y, Tanabe Y, Ishii K. Stretch-induced contraction of rabbit isolated pulmonary artery and the involvement of endothelium-derived thromboxane A_2. *Br J Pharmacol*. 1997;122(2):199-208.

46. Pak O, Janssen W, Ghofrani HA, Seeger W, Grimminger F, Schermuly RT, et al. Animal models of pulmonary hypertension: role in translational research. Drug Discov Today Dis Models. 2010;7(3-4):89-97.

47. Paravicini TM, Montezano AC, Yusuf H, Touyz RM. Activation

of vascular p38MAPK by mechanical stretch is independent of c-Src and NADPH oxidase: influence of hypertension and angiotensin II. *J Am Soc Hypertens*. 2012;6(3):169-78.

48. Park KS, Kim Y, Lee YH, Earm YE, Ho WK. Mechanosensitive cation channels in arterial smooth muscle cells are activated by diacylglycerol and inhibited by phospholipase C inhibitor. *Circ Res.* 2003;93(6):557-64.

49. Park KS, Lee HA, Earm KH, Ko JH, Earm YE, Kim SJ. Differential distribution of mechanosensitive nonselective cation channels in systemic and pulmonary arterial myocytes of rabbits. *J Vasc Res*. 2006;43(4):347-54.

50. Park SJ, Yoo HY, Earm YE, Kim SJ, Kim JK, Kim SD. Role of arachidonic acid-derived metabolites in the control of pulmonary arterial pressure and hypoxic pulmonary vasoconstriction in rats. *Br J Anaesth*. 2011;106(1):31-7.

51. Sedoris KC, Ovechkin AV, Gozal E, Roberts AM. Differential effects of nitric oxide synthesis on pulmonary vascular function during lung ischemia-reperfusion injury. *Arch Physiol Biochem*. 2009;115(1):34-46.

52. Song P, Zhang M, Wang S, Xu J, Choi HC, Zou MH. Thromboxane A_2 receptor activates a Rho-associated kinase/LKB1/PTEN pathway to attenuate endothelium insulin signaling. *J Biol Chem*. 2009;284(25):17120-8.

53. Thacher TN, Silacci P, Stergiopulos N, da Silva RF. Autonomous effects of shear stress and cyclic circumferential stretch regarding endothelial dysfunction and oxidative stress: an ex vivo arterial model. *J Vasc Res*. 2010;47(4):336-45.

54. Thomas SR, Chen K, Keaney JF, Jr. Hydrogen peroxide activates endothelial nitric-oxide synthase through coordinated phosphorylation and dephosphorylation via a phosphoinositide 3-kinase-dependent signaling pathway. *J Biol Chem*. 2002;277(8):6017-24.

55. Tosun M, Paul RJ, Rapoport RM. Role of extracellular Ca^{2+} influx via L-type and non-L-type Ca^{2+} channels in thromboxane A_2 receptor-mediated contraction in rat aorta. *J Pharmacol Exp Ther.* 1998;284(3):921-8.

56. Tran QK, Leonard J, Black DJ, Nadeau OW, Boulatnikov IG, Persechini A. Effects of combined phosphorylation at Ser-617

and Ser-1179 in endothelial nitric-oxide synthase on EC50(Ca^{2+}) values for calmodulin binding and enzyme activation. *J Biol Chem*. 2009;284(18):11892-9.

57. West JB. Pulmonary physiology and pathophysiology: an integrated, case-based approach. 2nd ed. Philadelphia: Wolters Kluwer Health/Lippincott Williams & Wilkins; 2007. vii, 150 p.

58. Yoo HY, Kim SJ. Disappearance of hypoxic pulmonary vasoconstriction and O_2-sensitive nonselective cationic current in arterial myocytes of rats under ambient hypoxia. *Korean J Physiol Pharmacol*. 2013;17(5):463-8.

59. Yoo HY, Park SJ, Seo EY, Park KS, Han JA, Kim KS, et al. Role of thromboxane A_2-activated nonselective cation channels in hypoxic pulmonary vasoconstriction of rat. *Am J Physiol Cell Physiol*. 2012;302(1):C307-17.

60. Zhou X, Yuan D, Wang M, He P. H_2O_2-induced endothelial NO production contributes to vascular cell apoptosis and increased permeability in rat venules. *Am J Physiol Heart Circ Physiol*. 2013;304(1):H82-93.

국문 초록

폐동맥압 (평균 12 mmHg)은 체동맥압 (평균 90 mmHg)에 비하여 현저히 낮으며, 폐순환계의 말초저항 또한 낮게 유지된다. 폐동맥의 유순도는 높아서, 폐혈류 증가 시 혈압변동은 낮게 유지될 수 있다. 또한 폐동맥은 신전감수성양이온통로 (SAC)가 존재함에도 불구하고 근원성 수축반응이 관찰되지 않는다. 평활근 이완 조절에 중요한 eNOS 가 폐동맥 평활근세포에 발현된다면 폐동맥의 낮은 긴장도를 설명할 수 있다는 가설을 바탕으로 아래 연구를 수행하였다.

박리한 백서 폐동맥 (PA) 절편의 수축장력을 측정하였다. 내피세포가 제거된 PA 절편의 피동적 신전상태가 높은 (0.3 g) 조건 (S(+))에서 thromboxane A_2 (TXA_2) 유사물질 U46619 (5 nM) 투여는 뚜렷한 수축을 일으키지 않았다. 하지만 NOS 억제제인 L-NAME 추가 투여는 큰 수축을 일으켰다 (80K 수축의 96 %). 피동적 신전상태가 낮은 (0.1 g) 조건 (S(-))에서는 U46619 와 L-NAME 투여에 의한 수축 (TXA_2/L-NAME 수축)은 현저히 낮았다 (80K 수축의 21%). nNOS 나 iNOS 특이적 억제제는 수축반응을 일으키지 못하였으므로, eNOS 가 TXA2/L-NAME 수축반응에 중요한 표적임을 알 수 있었다. 장간막 동맥과 신장 동맥은 피동적 신전이 높은 상태에서 TXA_2/L-NAME 수축반응을 뚜렷이 보이지 않았다. 폐동맥

평활근세포에서 eNOS 의 mRNA 발현과 단백질 발현을 확인하였다.

SAC 억제제들 (GxMTx4, DIDS) 전처치는 S(+) PA 에서의 TXA2/L-NAME 수축을 차단하였다. 폐동맥 평활근세포에 대한 팻취클램프 실험을 통하여 SAC 의 활성조건을 분석하였을 때, 세포막 신전자극에 더하여 H_2O_2 투여 시 활성 빈도가 유의하게 증가하였다. 흥미롭게도 S(-) PA 에 H_2O_2 (0.1-10 μM) 추가투여는 TXA_2/L-NAME 수축을 S(+) PA 의 반응만큼 증강시켰다. NADPH oxidase 억제제 (VAS2870 과 Apocynin)와 활성산소 제거제 (Tiron 과 PEG-catalase)들은 모두 S(+) PA 에서 TXA_2/L-NAME 수축을 유의하게 약화시켰다. 활성산소가 일으키는 하부 신호계의 하나인 Akt 의 억제제 (sc-66) 또한 S(+) PA 에서 TXA_2/L-NAME 수축을 약화시켰다. 인간 폐동맥 평활근세포주에서 eNOS 단백질 발현을 확인하였다. U46619 와 H_2O_2 는 eNOS 의 세린 1177 잔기 인산화를 일으켰고, 같은 세포주에서 U46619 는 Akt 의 세린 473 잔기 인산화를 일으켰다.

위의 실험에서 발견한 폐동맥 평활근의 eNOS 는 H_2O_2 와 Akt 신호전달을 매개로 하여 TXA_2 와 신전 자극에 의해 활성화 되는 것으로 보인다. 폐동맥 평활근에 존재하는 eNOS 는 폐순환계 특유의 낮은 압력 유지에 도움이 될 것으로 해석된다. 한편, monocrotaline 투여 또는 만성 저산소 사육조건에서 유발되는 폐동맥고혈압 백서 모델에서 박리한 폐동맥들은 TXA_2/L-NAME 수축이 유의하게 감소하였다. 이는 폐동맥 평활근에 발현된 eNOS 의 병태생리적 중요성을 시사한다.

주요어: 폐동맥 평활근세포, 내피세포형 산화질소 합성효소, 신전자극, 트롬복산 A_2, 과산화수소

학 번 : 2011-21938